https://doi.org/10.5194/amt-2020-63
Preprint. Discussion started: 6 March 2020

Atmospheric Measurement Techniques Discussions

1.5 years of TROPOMI CO measurements: Comparisons to MOPITT and ATom

Sara Martínez-Alonso[1], Merritt Deeter[1], Helen Worden[1], Tobias Borsdorff[2], Ilse Aben[2], Róisin Commane[3], Bruce Daube[7], Gene Francis[1], Maya George[4], Jochen Landgraf[2], Debbie Mao[1], Kathryn McKain[5,6], and Steven Wofsy[7]

[1]Atmospheric Chemistry Observations and Modeling (ACOM), National Center for Atmospheric Research(NCAR), Boulder, CO, USA
[2]SRON Netherlands Institute for Space Research, Utrecht, Netherlands
[3]Lamont-Doherty Earth Observatory, Columbia University, NY, USA
[4]LATMOS/IPSL, Sorbonne University, UVSQ, CNRS, Paris, France
[5]Cooperative Institute for Research in Environmental Sciences (CIRES), University of Colorado, Boulder, CO, USA
[6]Earth System Research Laboratory, Global Monitoring Division (GMD), National Oceanic and Atmospheric Administration, Boulder, CO, USA
[7]School of Engineering and Applied Science and Department of Earth and Planetary Sciences, Harvard University, Cambridge, MA, USA

Correspondence: Sara Martínez-Alonso (sma@ucar.edu)

Abstract. We have analyzed TROPOspheric Monitoring Instrument (TROPOMI) carbon monoxide (CO) data acquired between November 2017 and March 2019 with respect to other satellite (MOPITT, Measurement Of Pollution In The Troposphere) and airborne (ATom, Atmospheric Tomography mission) datasets to understand better TROPOMI's contribution to the global tropospheric CO record (2000 to present). TROPOMI and MOPITT are currently the only satellite instruments deriving CO from solar reflected radiances. Therefore, it is particularly important to understand how these two datasets compare. Our results indicate that TROPOMI CO retrievals over land show excellent agreement with respect to MOPITT: relative biases and their standard deviation (i.e., accuracy and precision) are on average -3.73 $\pm$ 11.51, -2.24 $\pm$ 12.38, and -3.22 $\pm$ 11.13 %, compared to the MOPITT TIR (thermal infrared), NIR (near infrared), and TIR+NIR (multispectral) products, respectively. TROPOMI and MOPITT data also show good agreement in terms of temporal and spatial patterns.

Despite depending on solar reflected radiances for its measurements, TROPOMI can also retrieve CO over bodies of water if clouds are present, by approximating partial columns under cloud tops using scaled, model-based reference CO profiles. We quantify the bias of TROPOMI total column retrievals over bodies of water with respect to colocated *in situ* ATom CO profiles after smoothing the latter with the TROPOMI column averaging kernels (AK), which account for signal attenuation under clouds (relative bias and its standard deviation = 3.25 $\pm$ 11.46 %). In addition, we quantify e_{null} (the null-space error), which accounts for differences between the shape of the TROPOMI reference profile and that of the ATom true profile (e_{null} = 2.16 $\pm$ 2.23 %). For comparisons of TROPOMI and MOPITT retrievals over open water, we adopt a simpler approach, since smoothing with TROPOMI AK does not apply for MOPITT retrievals. To this effect, we compare TROPOMI total CO columns (above and below cloud tops) and partial CO columns (above cloud top) to their colocated MOPITT TIR counterparts. (This approximation

https://doi.org/10.5194/amt-2020-63
Preprint. Discussion started: 6 March 2020

Atmospheric Measurement Techniques Discussions

would be most accurate for optically thick clouds.) We find very small changes in relative bias between TROPOMI and MOPITT TIR retrievals if total columns are considered instead of partial above-cloud-top columns (<1 percentage point).

https://doi.org/10.5194/amt-2020-63
Preprint. Discussion started: 6 March 2020

Atmospheric Measurement Techniques Discussions

1 Introduction

Even though carbon monoxide (CO) constitutes less than one millionth of the troposphere in volume, it is of great importance to understand climate and to monitor and predict air quality. Tropospheric CO is produced by incomplete fuel combustion, biomass burning, and oxidation of methane and other hydrocarbons. CO's main sink is oxidation by the hydroxyl radical (OH) (Spivakovsky et al., 2000; Lelieveld et al., 2016); this reaction produces greenhouse gases such as carbon dioxide and tropospheric ozone. Additionally, OH engaged in reactions with CO is not available to scavenge other greenhouse gases such as methane, which then have a longer lifetime in the atmosphere. As a consequence, CO emissions have a positive indirect radiative forcing of 0.23 W/m^2 (Myhre et al., 2013). The mean lifetime of tropospheric CO (variable by season and latitude, in addition to other factors; Holloway et al., 2000) is approximately 2 months. Because of its average lifetime, -long enough to last through horizontal and vertical transport and, yet, short enough not to become well mixed-, it is often used as a tracer to monitor the distribution, transport, sources, and sinks of polluted plumes (e.g., Heald et al., 2003). A self-consistent, uninterrupted record of global tropospheric CO is, thus, key to both climate and air quality studies. The aim of this work is to facilitate the extension of the current satellite record with newly available TROPOMI data by evaluating those with respect to MOPITT satellite and ATom aircraft *in situ* data.

The pre-launch targets for TROPOMI total CO column accuracy and precision were 15 and 10 %, respectively, for both clear and low-altitude-cloud observations (Veefkind et al., 2012; Landgraf et al., 2016). Retrieval errors are expected to be larger for cloudy conditions due to several effects, including the shape of model-based reference profiles (Borsdorff et al., 2018b). Global comparisons of TROPOMI retrievals with respect to ECMWF/IFS (European Center for Medium-Range Weather Forecast/Integrated Forecasting System) CO assimilation results (which incorporate CO retrievals from MOPITT as well as from IASI, the Infrared Atmospheric Sounding Interferometer (Clerbaux et al., 2009)) showed a relative high bias of 3.2 % with standard deviation of 5.5 % (Borsdorff et al., 2018a). TROPOMI CO retrievals over land have also been previously compared to ground-based measurements from nine TCCON (Total Carbon Column Observing Network) stations for selected dates between 9 November 2017 and 4 January 2018; good agreement between both datasets was found, with the TROPOMI CO product well within the mission requirements (Borsdorff et al., 2018b). Here we analyze daily global TROPOMI retrievals acquired between 7 November 2017 and 10 March 2019 with respect to satellite (MOPITT, Measurements Of Pollution In The Troposphere) and airborne (ATom, Atmospheric Tomography mission) CO datasets.

MOPITT is the only currently operating satellite instrument deriving CO from near-infrared (NIR), thermal-infrared (TIR), and multispectral (TIR+NIR) radiances; also, it has the longest global CO record to date (2000-present). Because TROPOMI is the only other satellite instrument retrieving CO from NIR measurements, understanding how MOPITT and TROPOMI retrievals compare to each other is key. MOPITT results are systematically validated using airborne vertical profiles (Deeter et al., 2019, and references therein) and ground measurements (Buchholz et al., 2017; Hedelius et al., 2019), as well as compared

https://doi.org/10.5194/amt-2020-63
Preprint. Discussion started: 6 March 2020


Atmospheric Measurement Techniques Discussions

to other satellite datasets (Worden et al., 2013a; Martínez-Alonso et al., 2014; George et al., 2015). Thus, its continuity and consistency are well understood.

Despite the low reflectivity of open water, TROPOMI CO retrievals over bodies of water are possible if clouds are present. In these cases partial CO columns under the cloud tops are approximated by scaled TROPOMI reference profiles (Borsdorff et al., 2018b). We quantify the error introduced by this approach by comparing TROPOMI CO retrievals over bodies of water to both airborne ATom-4 (fourth ATom campaign) and MOPITT TIR data.

Next we describe the datasets used (Sect. 2), detail how comparisons were performed (Sect. 3), present results from these comparisons (Sect. 4), discuss their significance (Sect. 5), and offer conclusions (Sect. 6). Additional results are available in the Supplement Materials.

2 Data

2.1 TROPOMI

TROPOMI is a push-broom imaging spectrometer on board ESA's Sentinel-5 Precursor platform, flying in a sun-synchronous orbit at 824 km altitude and 13:30 LST (local standard time) Equator crossing time. Its swath width of 2600 km allows for global daily coverage at very high spatial resolution, with a 7.2 x 7.2 km^2 footprint at nadir (Veefkind et al., 2012). (A change in the Copernicus Sentinel-5P operations scenario postdating the work presented here has resulted in a 7.2 x 5.6 km^2 footprint at nadir, starting 6 August 2019.) TROPOMI measures radiances in the ultraviolet, visible, and solar reflected infrared. Total CO column values are obtained from measurements of reflected solar infrared radiation in the 2.3 μm spectral range (Landgraf et al., 2016), corresponding to the first overtone of the CO stretch fundamental. Over land, retrievals are performed in both clear and cloudy conditions. Because of the low reflectivity of open water, retrievals over bodies of water are performed only in cloudy conditions.

TROPOMI CO retrievals are based on SICOR (Shortwave Infrared Carbon Monoxide Retrieval) (Vidot et al., 2012). In this physics-based algorithm, the retrieval state vector includes a single scaling factor representing the ratio of the retrieved CO profile to the reference CO profile (Borsdorff et al., 2014). Reference profiles are generated with the global chemical transport model TM5 (Krol et al., 2005); they are variable with respect to location, month, and year. Retrieved total CO column values simply correspond to the vertically-integrated CO profile. Over land, in the absence of clouds, the TROPOMI total CO column averaging kernel (AK; Fig. 1) is near unity over the entire vertical profile (Landgraf et al., 2016). Thus, clear-sky total CO column retrievals are negligibly affected by either the actual vertical distribution of CO or the shape of the CO reference profile. In the presence of clouds, however, over both land and bodies of water, the total CO column retrievals are mainly sensitive to the above-cloud CO partial column. The lack of sensitivity to the below-cloud CO partial column is compensated by increasing the sensitivity to the above-cloud CO partial column. Clouds thus lead to total column AK values greater than one above the cloud decreasing towards zero below the cloud (Landgraf et al., 2016).

https://doi.org/10.5194/amt-2020-63
Preprint. Discussion started: 6 March 2020


Atmospheric Measurement Techniques Discussions

The earliest TROPOMI CO retrievals date from 7 November 2017; therefore, this is the initial date of the period we analyze here. For any given day, we used either OFFL (offline) or RPRO (reprocessed) files, all from Collection 01, and from the most recent processor version available (10001, 10002, 10100, 10200, 10202, 10301, or 10302).

Retrievals were filtered as follows. The two most westward pixels in each granule were removed to avoid artifacts from unresolved calibration issues (Borsdorff et al., 2018a, b); daytime only observations were selected by keeping those with solar zenith angle <80°. Quality flag values (QA) were used to preserve clear-sky and clear-sky-like observations over land (QA = 1, corresponding to optical thickness <0.5 and cloud height <500 m) or observations with mid-level clouds over bodies of water (QA = 0.5; optical thickness $\geq$ 0.5 and cloud height <5000 m) (Landgraf et al., 2018).

2.2 MOPITT

MOPITT is a cross-track scanning gas correlation radiometer on board NASA's Terra satellite (Drummond and Mand, 1996; Drummond et al., 2010; Worden et al., 2013b). Terra is in a sun-synchronous orbit at 705 km altitude and 10:30 LST Equator crossing time. MOPITT has horizontal resolution near 22 x 22 km^2 at nadir and a swath width of 640 km; global coverage is achieved in approximately 3 days. MOPITT observations enable retrievals of tropospheric CO vertical profiles and corresponding total column amounts from both TIR and NIR measurements in the spectral regions where the fundamental (~4.7 μm) and first overtone (~2.3 μm) of the CO stretch occur, respectively. TIR measurements are useful over both bodies of water and land, day and night; NIR radiances only in daytime observations over land. MOPITT CO retrieval products are available in three variants (TIR-only; NIR-only; and TIR+NIR, or multispectral) characterized by different vertical sensitivity and random retrieval noise (Deeter et al., 2019, and references therein).

Unlike TROPOMI's, the MOPITT retrieval algorithm relies on optimal estimation whereby *a priori* information constrains the retrieved profile in the absence of information from the measured radiances (Deeter et al., 2003). MOPITT *a priori* profiles vary seasonally and geographically according to a multi-year (2000-2009) Community Atmosphere Model with Chemistry (CAM-Chem) model-based CO climatology (Lamarque et al., 2012). MOPITT profile retrievals are performed on a ten-level pressure grid; the reported retrieval for each level indicates the mean volume mixing ratio (VMR) in the layer immediately above that level. Reported total CO column values are obtained by integrating the retrieved VMR profiles from the surface to the top of the atmosphere. Internally, CO concentrations in the retrieval state vector are represented in terms of the logarithm of the VMR. For each retrieved CO profile, both the full retrieval AK matrix and total column AK are produced simultaneously and are provided as diagnostics. As indicated by the AK (Fig. 1), sensitivity characteristics of the three products are quite different (Deeter et al., 2012). With respect to vertical sensitivity, total column AK for the NIR-only product are most similar in shape to the TROPOMI total column AK, but NIR retrievals can be significantly constrained by the *a priori*. In comparison, TIR-only total column AK exhibit weaker sensitivity to CO near the surface, but TIR retrievals are less strongly weighted by the *a priori* overall. TIR+NIR total column AK are typically more uniform than for TIR-only retrievals, although the benefits of combining TIR and NIR measurements are only apparent in daytime observations over land.

Here we use daytime archive MOPITT data from version 8 (Deeter et al., 2019). The MOPITT retrieval algorithm processes only clear-sky observations (Francis et al., 2017). The clear/cloudy status of an observation is typically determined from

https://doi.org/10.5194/amt-2020-63
Preprint. Discussion started: 6 March 2020


Atmospheric Measurement Techniques Discussions

MOPITT radiances as well as a cloud mask (Ackerman et al., 1998) based on simultaneous observations by MODIS (MODerate resolution Imaging Spectroradiometer, also on board the Terra platform). MODIS observations (~480; note 1 km resolution) acquired at the same time as a single MOPITT observation and within the MOPITT footprint are identified and collected; relevant MODIS cloud descriptors (available in the MOPITT L2 product) are evaluated. MOPITT observations for which at least 95% of the colocated MODIS cloud mask values are considered clear are passed to the retrieval algorithm. MOPITT archive data are those corrected with gain and offset values derived from an interpolation performed between two consecutive hot-calibration events, which are usually executed once per year. This retrospective correction alleviates large differences in total column values otherwise observed in NIR retrievals; TIR products are affected to a much lesser degree (Deeter et al., 2017). Here we use MOPITT archive data produced after the hot calibration performed between 11 and 23 March 2019; thus, the closing date for the period analyzed here is 10 March 2019. Total column validation results for version 8 products indicate that relative biases and standard deviations are less than 1 and 7 %, respectively (i.e., less than 0.5 and 1.5 x 10^{17} molec. cm^{-2}) (Deeter et al., 2019).

2.3 ATom-4

To analyze TROPOMI retrievals over bodies of water we use ATom (Wofsy et al., 2018) *in situ* CO profiles from its fourth campaign, carried out between 24 April and 21 May 2018. During ATom-4 more than 150 vertical profiles were acquired, most of them over water in the Atlantic and Pacific regions, and covering a wide latitudinal range. CO concentrations along those profiles were measured with the Harvard QCLS (pulsed-Quantum Cascade Laser System) instrument (Santoni et al., 2014; McManus et al., 2010) and the NOAA Picarro Cavity Ring Down Spectrometer (Crosson, 2008; Karion et al., 2013), both on board NASA's DC-8 platform. Measurements were acquired from 0.2 to 12 km altitude at 1 Hz sampling rate. The QCLS instrument operates in the 4.59 μm region, with precision and accuracy of 0.15 and 3.5 ppb, respectively (Santoni et al., 2014). The NOAA Picarro measures radiation in the 1.57 μm region, where the second overtone of the CO stretch is located; the estimated total uncertainty of its measurements is 5.0 ppb at 1 Hz, or 3.4 ppb at 0.1 Hz (McKain and Sweeney, 2018). Here we use the merged QCLS-Picarro data product CO.X from the dataset version published 28 March 2018 and updated 25 November 2019. The quantity CO.X uses QCLS CO data with calibration gaps filled in by Picarro CO data, after subtracting the low-pass filtered difference between the QCLS and the somewhat noisier Picarro measurement. Both instruments were calibrated to the NOAA X2014A CO scale. Measurements account for drift of CO in their field calibration tanks (ESRL, 2018) by having them measured at the central calibration laboratory before and after the campaign and applying a linear drift correction to the assigned values.

https://doi.org/10.5194/amt-2020-63
Preprint. Discussion started: 6 March 2020


Atmospheric Measurement Techniques Discussions

3 Methods

3.1 Land retrieval comparisons

To validate TROPOMI land CO retrievals, we selected six ROIs (regions of interest; Fig. 2) representative of either polluted or clean regimes. Polluted ROIs include: south-eastern USA (thereafter referred to as USA; 35°N, 95°W to 40°N, 75°W), central Europe (Europe; 45°N, 0°E to 55°N, 15°E), northern half of the Indian Subcontinent (India; 20°N, 70°E to 30°N, 95°E), and north-eastern China (China; 30°N, 110°E to 40°N, 123°E). Clean ROIs are: northern Africa and Arabia (Sahara; 15°N, 20°W to 30°N, 50°E) and western Australia (Australia; 32°S, 112°E to 17°S, 138°E). Two additional ROIs were defined to represent most of the northern and southern (N and S) hemispheres (0°N to 60°N and 60°S to 0°N, respectively).

TROPOMI and MOPITT retrievals covering each of these ROIs for the period between 7 November 2017 and 10 March 2019 were gathered and filtered to keep only clear daytime data over land. According to Rodgers and Connor (2003), comparisons of remote sounder retrievals obtained with optimal estimation-based methods must take into account the differences of the observation systems (e.g., AK and *a priori*). However, as discussed earlier, TROPOMI uses a method which scales the reference profiles such that the retrieved total columns are independent of them (Borsdorff et al., 2014; Landgraf et al., 2016). Therefore, because the Rodgers and Connor (2003) methodology is not applicable in this case, MOPITT and TROPOMI total column retrievals are compared here without any transformation.

Colocated and non-colocated retrievals from the two instruments were analyzed separately; results from the former are presented in the following sections, supporting results from the latter in the Supplement Materials. We apply the term 'colocated' to pairs of retrievals from two different datasets acquired on the same day and within $\leq$ 50 km in horizontal distance. In contrast, we apply the term 'non-colocated' to retrievals from two different datasets acquired on the same day and inside the same ROI. Colocated samples allow for a more direct comparison, since they are more closely representative of the same atmospheric conditions. By using non-colocated retrievals we maximized the size and diversity of the populations analyzed.

Daily scatterplots for each ROI were obtained from the colocated retrievals. We quantified, among others, daily bias (i.e., accuracy) and standard deviation (i.e., precision) between TROPOMI and each of the three MOPITT products (TIR, NIR, and TIR+NIR). Relative bias values (in %) were calculated with respect to MOPITT in all cases (100x(TROPOMI-MOPITT)/MOPITT). Column bias values (in molec. cm^{-2}), also provided for completeness, were calculated with respect to MOPITT (TROPOMI-MOPITT). Thus, a negative bias would indicate that TROPOMI CO values are lower than their MOPITT counterparts.

3.2 Water retrieval comparisons

TROPOMI CO retrievals over bodies of water are possible if clouds are present in the field of view (Landgraf et al., 2016); otherwise, because of the low reflectivity of open water to shortwave infrared solar radiation, insufficient radiance would be available for the instrument to measure. TROPOMI retrievals are achieved by estimating the altitude of the cloud top from the difference between measured and modeled methane, as described in Landgraf et al. (2016), and then approximating the partial CO column under the cloud top by the colocated, scaled TROPOMI reference profile partial column. For validating

https://doi.org/10.5194/amt-2020-63
Preprint. Discussion started: 6 March 2020


Atmospheric Measurement Techniques Discussions

TROPOMI total column retrievals over bodies of water, we performed separate comparisons with *in-situ* profiles from the ATom-4 campaign and with MOPITT TIR-only retrievals. Given their nature, all comparisons over bodies of water used colocated observations.

3.2.1 TROPOMI versus ATom-4: AK analysis

In-situ profile data acquired from aircraft are well-suited for validating satellite CO retrievals. To validate TROPOMI retrievals over bodies of water, we derived both true and retrieval-simulated (i.e., unsmoothed and smoothed) total CO column values from the ATom-4 profiles; smoothed values account for the vertical sensitivity of the TROPOMI measurements as expressed by their AK.

Prior to obtaining unsmoothed/smoothed ATom-4 total CO columns, complete (e.g., from the surface to the top of the atmosphere) ATom-4 CO profiles were generated following the standard method for MOPITT validation with airborne data. Profiles that did not cover the 400-to-800 hPa range were rejected. The remaining profiles (between 271 $\pm$ 48 hPa and 983 $\pm$ 32 hPa) were interpolated to match the MOPITT *a priori* 35-level vertical grid, which preserves high vertical resolution in the troposphere. Empty levels at the bottom of each interpolated profile (levels with no CO value) were filled with the interpolated measurement closest to the surface. Similarly, empty levels between the top of the interpolated profile and the tropopause were filled with the interpolated measurement closest to the tropopause. Finally, empty levels above the tropopause were filled with colocated MOPITT *a priori* CO values. Unsmoothed ATom-4 total CO column values were then calculated as follows:

$$C = 2.12 * 10^{13} \sum_{i=1}^{i=n} \Delta p_i x_i \quad (1)$$

where C is the total column value in molec. cm^{-2}, n is the number of partial columns in the profile, Δp_i is the thickness of partial column i in hPa, and x_i is the mean VMR for the layer above level i reported in ppbv units. The derivation of Eq. (1) can be found in Deeter (2009).

Smoothed ATom-4 total CO column values involve the TROPOMI AK, which are provided with the actual total column retrievals. In cloudy scenes, TROPOMI total column retrievals are more sensitive to CO above the cloud than to CO below the cloud; smoothed total column values account for this effect explicitly. As shown in Borsdorff et al. (2014) and Landgraf et al. (2016), the relation between the retrieved TROPOMI total column $\hat{c}$ and the true CO profile ρ^{true} (a vector of CO partial column values rather than VMR values) can be expressed as

$$\hat{c} = A^{col} \rho^{true} + \epsilon_x \quad (2)$$

where A^{col} is the TROPOMI column AK and ϵ_x is the retrieval error. Thus, smoothed ATom-4 CO profiles can be calculated using

$$c^{sim} = A^{col} \rho^{true} \quad (3)$$

https://doi.org/10.5194/amt-2020-63
Preprint. Discussion started: 6 March 2020


Atmospheric Measurement Techniques Discussions

and substituting ρ^{true} by the the complete ATom-4 profiles obtained as detailed above and interpolated to match the 50-level vertical grid of their colocated TROPOMI total column AK. Finally, smoothed ATom-4 total CO column values are calculated applying Eq. (1).

Comparisons between TROPOMI total column retrievals and true (unsmoothed) ATom-4 total column values are the most direct, but they are subject to various sources of random and systematic error. Comparisons between TROPOMI total column retrievals and retrieval-simulated (smoothed) ATom-4 column values should be less affected by TROPOMI vertical sensitivity variations, and can be used to investigate the overall performance of the retrieval. Relative bias values were calculated with respect to ATom in all cases (100x(TROPOMI-ATom)/ATom); column bias values too (TROPOMI-ATom).

In addition, we quantified the error introduced by approximating the partial column below cloud top with the TROPOMI reference profile by calculating the null-space error of the TROPOMI retrieval process (e_{null}) as described in Borsdorff et al. (2014) and Landgraf et al. (2016):

$$e_{null} = (I - A^{col})\rho^{true} \tag{4}$$

where *I* is the altitude integral operator. As discussed in Sect. 4.2.1, analysis of e_{null} may be useful for diagnosing retrieval errors over cloudy scenes related to the shape of the TROPOMI model-calculated reference profiles.

3.2.2 TROPOMI versus MOPITT TIR: above/below cloud analysis

For this comparison we assumed that TROPOMI retrievals are only sensitive to CO above cloud top, while CO below cloud top is fully approximated by TROPOMI's scaled reference profiles. This scenario would be most accurate in case of optically thick clouds. To quantify the error introduced by approximating below-cloud-top CO with TROPOMI reference profiles, we compared TROPOMI retrievals over bodies of water (total columns and their above cloud partial column components) to their colocated MOPITT TIR counterparts. For each TROPOMI observation, a partial above cloud column was calculated by subtracting from the reported total TROPOMI column the below cloud partial column of its colocated, scaled TROPOMI reference profile, available in a 25-level vertical grid. Scaling factors produced in the TROPOMI retrieval process are not included in the TROPOMI product; we obtained those by dividing each reported TROPOMI total CO column retrieval by the total CO column of its colocated reference profile, calculated using Eq. (1). Total and partial above cloud column values were also calculated for the colocated MOPITT TIR profiles interpolated to match the 25-level vertical grid of the reference profiles. The same analysis was performed using colocated TROPOMI and ATom-4 data; results are available in the Supplement Materials.

4 Results

Land-only comparisons have the purpose of evaluating TROPOMI's performance with respect to MOPITT TIR, NIR, and TIR+NIR. Separate comparisons were performed using either colocated data (results in Sect. 4.1) or non-colocated data (Supplement Materials). Water-only comparisons aim to estimate the error introduced in TROPOMI retrievals over bodies of water,

https://doi.org/10.5194/amt-2020-63
Preprint. Discussion started: 6 March 2020


Atmospheric Measurement Techniques Discussions

only possible in cloudy conditions, by approximating CO concentrations below cloud top by colocated, scaled TROPOMI reference profile values. Two sets of water-only comparisons were performed. First, with respect to *in situ* ATom-4 profiles, accounting for differences in TROPOMI vertical sensitivity as represented by its AK (4.2.1). Second, with respect to MOPITT TIR (4.2.2) and ATom-4 profiles (Supplement Materials) assuming a simple scenario where TROPOMI only had sensitivity to CO above cloud top.

4.1 TROPOMI retrievals over land

Here we describe results from the comparison of daily (from 7 November 2017 to 10 March 2019) colocated TROPOMI and MOPITT retrievals over 8 ROIs: 2 hemispheric, 4 representative of polluted regions, and 2 of clean regions (Fig. 2). Daily bias and standard deviation values calculated between TROPOMI and each of the three MOPITT products are presented below.

4.1.1 TROPOMI versus MOPITT TIR

Daily results from the analysis of colocated TROPOMI and MOPITT TIR data (Fig. 3) show that during the ~1.5 years analyzed, TROPOMI and MOPITT TIR total CO column retrievals were close to each other both in magnitude and temporal variation. Both datasets agree in displaying strong differences between clean ROIs (Sahara and Australia; 10-20 x 10^{17} molec. cm^{-2}) and highly polluted ROIs (India and China; 15-40 x 10^{17} molec. cm^{-2}). They also show the expected differences between the two hemispheres: retrievals are, overall, lower in the S Hemisphere ROI (10-20 x 10^{17} molec. cm^{-2} versus 15-22 x 10^{17} molec. cm^{-2}) due to less land area, population, and industrial activity. Both TROPOMI and MOPITT TIR show similar seasonal variability. ROIs located in the northern hemisphere present an absolute maximum during boreal winter and a secondary maximum in late boreal summer. The absolute maximum is consistent with winter CO accumulation due to shorter days and (at high latitudes) larger solar zenithal angles resulting in less photolysis, and to increased emissions due to biomass burning north of the Equator in Africa. The secondary maximum is most likely due to fire emissions. Conversely, seasonal trends in southern hemisphere ROIs show a maximum in September-October, consistent with CO accumulation during austral winter and emissions from biomass burning S of the equator.

Daily relative bias values are generally within a ± 10 % range for all the ROIs except the two most polluted, India and China (Fig 3.e and 3.f), where biases reach higher values, mostly in the -20 to 20 % range. When averaged over time (Table 1), relative biases are between -8.15 % (Sahara) and 3.55 % (China), with a mean for all the ROIs of -3.73 %. We note that biases for most ROIs are predominantly negative, except for China, where most daily biases are positive. Averaged relative standard deviation values per ROI are between 6.05 and 16.04 % (USA and S Hemisphere, respectively), with a mean for all ROIs of 11.51 %.

4.1.2 TROPOMI versus MOPITT NIR

Figure 4 shows daily results from the comparison of colocated TROPOMI and MOPITT NIR land retrievals; time-averaged results are summarized in Table 1. The ranges of daily mean retrievals and seasonal trends observed in each ROI are in general analogous to those described in Sect. 4.1.1. Relative bias values averaged for the period analyzed range between -7.93 % (USA)

https://doi.org/10.5194/amt-2020-63
Preprint. Discussion started: 6 March 2020


Atmospheric Measurement Techniques Discussions

and 2.86 % (Sahara), while the mean for all the ROIs is -2.24 %. Daily relative bias values for the Sahara ROI (-5 to 12 % range; Fig. 4.g) differ strongly from those calculated with respect to MOPITT TIR (Fig. 3.g) (-12 to -5 % range). For all the other ROIs, relative biases with respect to MOPITT NIR are broadly similar in magnitude to those with respect to MOPITT TIR, albeit the former present larger oscillations with time. This is consistent with the MOPITT NIR retrievals being more sensitive to geophysical noise due to changes in albedo during a MOPITT observation associated with spacecraft motion (Deeter et al., 2011). Relative standard deviation values averaged over time are between 9.95 and 16.15 % (USA and China, respectively), with a mean for all ROIs of 12.38 %.

4.1.3 TROPOMI versus MOPITT TIR+NIR

Daily results from colocated TROPOMI and MOPITT TIR+NIR retrievals are shown in Fig. 5; time-averaged results are summarized in Table 1. Results are similar to those described in Sect. 4.1.1 in terms of daily mean retrieval values, retrieval seasonal trends, and relative biases. The latter range between -7.94 % (Sahara) and 4.53 % (China); the mean for all ROIs is -3.22 %. Averaged relative standard deviation values are between 6.48 % (Sahara) and 15.68 % (S Hemisphere), with a mean for all ROIs of 11.13 %.

4.2 TROPOMI retrievals over water

Next we present results from the comparison of colocated TROPOMI and ATom-4 retrievals between 24 April and 21 May 2018 over the Atlantic and Pacific regions. Similarly, we describe results obtained from colocated TROPOMI and MOPITT TIR over-water retrievals acquired between 7 November 2017 and 10 March 2019 over the two hemispheric ROIs. The ATom-4 data offer the opportunity to compare TROPOMI retrievals to *in situ* measurements; the MOPITT dataset has the advantage of a substantially larger number of samples, distributed over a longer period of time and a wider geographical area.

4.2.1 TROPOMI versus ATom-4: AK analysis

Results from the TROPOMI and ATom-4 comparison over bodies of water are summarized in Fig. 6 and Table 2. As described in Sect. 3.2.1, comparisons were performed both in terms of true (unsmoothed) and retrieval-simulated (smoothed) ATom-4 total column values; the latter account for the vertical sensitivity of the TROPOMI retrievals. Figure 6.a shows that unsmoothed ATom-4 total CO columns and TROPOMI are strongly correlated (R = 0.93, slope of linear fit = 0.96) and exhibit a negative relative bias (-4.76 %) indicative of low TROPOMI values with respect to the true ATom-4. In contrast, Fig. 6.b shows results for smoothed ATom-4 versus TROPOMI. The relative bias is in this case better (3.25 %) and the fit between the two datasets has a slightly larger R (0.94), indicative of an improved correlation. The slope of the linear fit is, however, slightly lower (0.90). Figure 7 shows the smoothed ATom-4 values in the context of TROPOMI; TROPOMI clearly captures the geographical patterns of the *in situ* measurements. Relative biases show no latitudinal dependence (Fig. 8).

As seen in Sect. 3.2.1, we can separately quantify the expected difference between the true total column and the TROPOMI retrieved total column due to the differences in shape between the true profile and the TROPOMI reference profile. In clear-sky

https://doi.org/10.5194/amt-2020-63
Preprint. Discussion started: 6 March 2020


Atmospheric Measurement Techniques Discussions

scenes (over land), the TROPOMI radiances fundamentally measure the integrated total column and the shape of the reference profile does not significantly affect the accuracy of the retrieved total column. In cloudy scenes (over land or water), however, the total column retrieval becomes more sensitive to above-cloud CO than to below-cloud CO; the validity of the reference profile shape acts in this case as a source of retrieval error. Values of the null-space error (e_{null}) calculated for each ATom-4 profile using Eq. (4) versus latitude are shown in Fig. 9. The relative mean and standard deviation values of e_{null} calculated with respect to true (unsmoothed) ATom-4 total columns are 2.16 $\pm$ 2.23 % (i.e., 3.70 $\pm$ 3.75 x 10^{16} molec. cm^{-2}). The prevalence of positive values for e_{null} indicates that, on average, the reference profiles analyzed have a slight tendency to have too much CO near the surface, resulting in an overestimate of the below-cloud partial column. No clear latitudinal dependence is observed in e_{null}.

4.2.2 TROPOMI versus MOPITT TIR: above/below cloud analysis

Figure 10 and Table 3 summarize results from our comparison of colocated TROPOMI and MOPITT TIR retrievals over bodies of water in the N Hemisphere ROI. The top panels in Fig. 10 illustrate a comparison between total column (above and below cloud top) and partial column (above cloud top) retrievals for a single day, 1 January 2018. Partial column values from TROPOMI and MOPITT are more strongly correlated in this particular date, as shown by a larger R (0.87 versus 0.73) and a smaller relative bias (2.77 versus 2.92 %). The bottom panels in Fig. 10 summarize similar daily results for the entire ~1.5-year period analyzed. Relative biases between TROPOMI and MOPITT TIR for total or partial columns are small (in the -2 to 11 % range, ~4 % on average) and follow the same temporal patterns; their differences (total column bias - partial column bias) range from -1.79 to 1.56 p.p. (percentage point), with a -0.53 p.p. mean. Standard deviation values are on average around 13-15 %.

Similar results for the S Hemisphere ROI are summarized in Fig. 11 and Table 3. Partial column values for 1 January 2018 (Fig. 11.b) have a larger R (0.84 versus 0.79) and appear more strongly correlated than their total column counterparts (Fig. 11.a). They, however, show a larger relative bias (2.16 versus 0.36 %). Similar results for the entire period analyzed (Fig. 11.c and .d) indicate that relative biases for either total or partial columns are similarly small, ranging from -5 to 7 (~3 % mean). Their differences are in the -3.62 to 0.97 p.p. range, with a -1.02 p.p. mean. Standard deviations are in the 18-21 % range.

Based on the difference in relative bias between the total (above and below cloud) and partial (above cloud) column analyses, we estimate that approximating TROPOMI CO below cloud top by scaled reference profiles results, on average, in a ~0.78 p.p. error. As explained in Sect. 3.2.2, this approach would be most accurate in the presence of optically thick clouds which would preclude TROPOMI sensitivity below cloud top.

5 Discussion

TROPOMI and MOPITT are consistent with each other in terms of the main spatial and seasonal CO features they capture, as shown by mean seasonal maps (Fig. 12). Both datasets display relatively high values in the Northern hemisphere during boreal winter (panels .a and .b) and spring (.c and .d), similarly high values during all seasons in Africa and Asia, and relatively

https://doi.org/10.5194/amt-2020-63
Preprint. Discussion started: 6 March 2020


Atmospheric Measurement Techniques Discussions

high values due to Amazon fires in austral summer and fall (.a and .b, .g and .h). We note differences between TROPOMI and MOPITT that we interpret as due to their contrasting daytime passing times (1:30PM and 10:30AM, respectively): TROPOMI shows higher CO over Africa than MOPITT, consistent with higher CO emissions from afternoon fires than from morning fires. (Fires are commonly more active in the afternoon than in the morning, as observed in fire counts from same day morning Terra MODIS versus afternoon Aqua MODIS (Giglio et al., 2006).) We also note that TROPOMI retrievals over Amazonia are lower than MOPITT's in all seasons. Identifying the reason for this discrepancy will require further investigation.

Quantitative results from the analysis of colocated TROPOMI and MOPITT land retrievals, summarized in Fig. 13 and Table 1, also show good agreement. Relative biases for all ROIs (-3.73 $\pm$ 11.51, -2.24 $\pm$ 12.38, and -3.22 $\pm$ 11.13 compared to MOPITT TIR, NIR, and TIR+NIR, respectively) are well within TROPOMI's required 15 % accuracy and close to 10 % precision target (Veefkind et al., 2012; Landgraf et al., 2016). We note that biases are mostly negative (i.e., TROPOMI retrievals are lower than MOPITT); further analyses would be needed to explain this observation. One exception is China, where biases are predominantly positive. Statistical results obtained from each of the three MOPITT products are consistent with each other for all the ROIs, except for the Sahara. In this case, relative biases between TROPOMI and MOPITT NIR are positive and closer to zero than biases between TROPOMI and TIR or TIR+NIR products. Results from non-colocated retrievals, available in the Supplement Section and summarized in Fig. 14, reinforce all these observations and provide additional insight.

Several factors may contribute to the contrasting results for the China ROI. First, because of its superior spatial resolution (7.2 x 7.2 km^2), TROPOMI can resolve small, highly polluted plumes which would appear diluted at MOPITT's 22 x 22 km^2 resolution. Second, TROPOMI provides daily global coverage, while MOPITT's return period is approximately three days; as a result, TROPOMI has more opportunities to sample highly polluted areas than MOPITT. Third, conservative MOPITT cloud mask rules may be responsible for fewer MOPITT retrievals over highly polluted regions, which are frequently hazy due to aerosols. Detailed daily maps (e.g., Fig. 15) obtained in the analysis of non-colocated observations indicate that MOPITT often fails to retrieve over highly polluted areas like Beijing (China). In this example many MOPITT observations, despite having been classified as cloud-free based on MOPITT radiances, were labeled cloudy (and no retrieval was performed) based on the MODIS cloud mask, which may be interpreting haze due to pollution or fire smoke as clouds. We note that comparisons of non-colocated retrievals are more strongly affected by these factors; this is consistent with particularly high positive biases derived from non-colocated retrievals over China (Fig. 14).

Possible causes for the contrasting relative biases obtained from the MOPITT NIR product over the Sahara include aerosol and/or surface albedo effects. Further work is needed to diagnose these effects for different wavelengths and to account for differences between MOPITT and TROPOMI measurement and retrieval methods. Determining the most accurate retrievals would require *in situ* CO column measurements (e.g., airborne profiles) that are not currently available for that region.

We have also analyzed daytime, colocated TROPOMI and ATom-4 data over the Atlantic and Pacific regions for the period between 24 April and 21 May 2018 to quantify the error introduced in TROPOMI retrievals over bodies of water (possible only under cloudy conditions) by approximating below-cloud-top partial columns with their colocated, scaled reference profiles. There is excellent agreement (-4.76 $\pm$ 11.15 % relative bias, i.e., below the mission requirement of 15 % accuracy and close to the 10 % precision target (Veefkind et al., 2012; Landgraf et al., 2016)) between ATom-4 total columns calculated from the true

https://doi.org/10.5194/amt-2020-63
Preprint. Discussion started: 6 March 2020


Atmospheric Measurement Techniques Discussions

(unsmoothed) *in situ* profiles and the reported TROPOMI total columns (Fig. 6.a). Retrieval-simulated ATom total CO column values are even closer to the TROPOMI retrievals (3.25 $\pm$ 11.46 % relative bias); this comparison accounts for the actual vertical sensitivity of the retrieval process as expressed in the TROPOMI AK, and summarizes the overall performance of the retrievals. The relative contributions of e_{null} with respect to true ATom-4 total CO columns are small (2.16 $\pm$ 2.23 %) and mostly positive, indicating a slight overestimate of the below-cloud partial column in the cases analyzed. No clear latitudinal dependence is observed in relative biases of total CO column or in e_{null}.

For an analysis of TROPOMI retrievals over bodies of water representative of a longer period of time (7 November 2017 to 10 March 2019) and larger region (N and S Hemisphere ROIs), we used MOPITT TIR observations in a simple above and below cloud approach which would be most accurate for optically thick clouds. Colocated TROPOMI and MOPITT TIR total CO columns (above and below cloud top) and their corresponding partial column (above cloud top) components were analyzed separately. We interpret the difference between total column and partial column relative biases (-0.78 p.p.) as an estimate of the error introduced by approximating below-cloud-top CO with TROPOMI reference profiles. A similar analysis using ATom-4 profiles instead of MOPITT TIR profiles, presented in the Supplement Materials, results in a -3.65 p.p. estimated error.

6 Conclusions

A consistent global record of tropospheric CO is important for climate studies as well as for air quality monitoring and prediction. To better understand TROPOMI in the context of the current CO satellite record and thus facilitate the record's extension, we have compared TROPOMI data to other satellite (MOPITT) and airborne (ATom) datasets. Our results show that the accuracy and precision of TROPOMI retrievals with respect to MOPITT and ATom satisfy Sentinel-5P mission requirements (Veefkind et al., 2012; Landgraf et al., 2016).

We have analyzed cloud-free, land-only TROPOMI and MOPITT retrievals from 7 November 2017 to 10 March 2019 over ROIs representative of clean, polluted, and hemispheric regions in order to compare total CO column values from the two instruments. ATom being restricted mostly to oceanic regions precludes the use of this *in situ* dataset for fully validating TROPOMI retrievals over land; to that end, *in situ* data from other airborne measurement programs are required. Quantitative comparisons between TROPOMI and MOPITT retrievals over land are relevant, nevertheless. The MOPITT dataset represents the longest global CO record available (2000-present); because of extensive validation efforts with respect to *in situ* measurements and other satellite datasets, it is well characterized. Additionally, MOPITT products have served as the reference for many other satellite retrieval products for CO, including AIRS (Worden et al., 2013b), TES (Worden et al., 2013b), and IASI (George et al., 2009, 2015). Furthermore, TROPOMI and MOPITT are currently the only satellite instruments retrieving CO from NIR solar-reflected radiances. Thus, it is important to understand their relative behavior, particularly because we are interested in continuing the MOPITT multispectral record (which has enhanced sensitivity to near surface CO for some land observations (Worden et al., 2010)) using radiances from TROPOMI (NIR) and SNPP-CrIS (TIR), two instruments on satellites flying in loose formation (Fu et al., 2016). While our TROPOMI-MOPITT comparisons do not fully account for the contrasting vertical sensitivities of these two instruments, their results show that there is excellent agreement between the two datasets.

https://doi.org/10.5194/amt-2020-63
Preprint. Discussion started: 6 March 2020


Atmospheric Measurement Techniques Discussions

To analyze TROPOMI retrievals over bodies of water, only possible in cloudy conditions, we have used both ATom-4 *in situ* data (24 April to 21 May 2018) and MOPITT TIR retrievals (7 November 2017 to 10 March 2019). The ATom comparison allowed full validation using the TROPOMI AK. This is the ideal situation, since retrieval-simulated ATom-4 column values (i.e., ATom-4 values smoothed using the TROPOMI AK) explicitly account for the TROPOMI retrieval vertical sensitivity (unlike TROPOMI/MOPITT comparisons). The MOPITT comparison provided useful information for a longer period and wider geographical extent, although with the same restrictions noted above regarding the land-only comparisons. Our analyses over bodies of water indicate that TROPOMI's use of reference profiles in cloudy conditions results in errors on the order of a few percent. Since there are no major CO sources over water, CO values closer to the surface (and, therefore, most likely to be below cloud top) tend to be spatially homogeneous and stable through time. Thus, they are well characterized by the reference profiles. Depending on the representativeness of the TROPOMI reference profiles, larger errors may occur in TROPOMI land retrievals under cloudy conditions, particularly near CO emission sources. These errors require further characterization with colocated *in situ* data over land.

Data availability. TROPOMI level 2 CO retrievals for the 7 November 2017 to 27 June 2018 were downloaded from https://s5pexp.copernicus.eu/; retrievals for dates after 28 June 2018 were downloaded from https://s5phub.copernicus.eu/. TROPOMI reference profiles were obtained from ftp://ftp.sron.nl/pub/jochen/TROPOMI_apriori/tm5_co/. MOPITT data can be downloaded from https://doi.org/10.5067/TERRA/MOPITT/MOP02T_L2.008 (TIR), MOP02N_L2.008 (NIR), and MOP02J_L2.008 (TIR+NIR). ATom-4 data from the 7 September 2019 version were downloaded from https://doi.org/10.3334/ORNLDAAC/1581.

Competing interests. The authors declare that they have no conflict of interest.

Acknowledgements. We thank Louisa Emmons and John Gille for providing helpful comments on this manuscript. This material is based upon work supported by the National Center for Atmospheric Research (NCAR), which is a major facility sponsored by the National Science Foundation under Cooperative Agreement No. 1852977. The NCAR MOPITT project is supported by the National Aeronautics and Space Administration (NASA) Earth Observing System (EOS) Program. Sentinel-5 Precursor is part of the EU Copernicus program, and Copernicus (modified) Sentinel data 2017-2019 has been used. TB is funded through the national TROPOMI program from the NSO. CO measurements on ATom were supported by NASA Earth Venture program through grants NNX15AJ23G to Harvard University and NNX16AL92A to the University of Colorado.

https://doi.org/10.5194/amt-2020-63
Preprint. Discussion started: 6 March 2020


Atmospheric Measurement Techniques Discussions

References

Ackerman, S., Strabala, K., Menzel, W., Frey, R., Moeller, C., and Gumley, L.: Discriminating clear sky from clouds with MODIS, JOURNAL OF GEOPHYSICAL RESEARCH-ATMOSPHERES, 103, 32 141–32 157, https://doi.org/10.1029/1998JD200032, 1998.

Borsdorff, T., Hasekamp, O. P., Wassmann, A., and Landgraf, J.: Insights into Tikhonov regularization: application to trace gas column retrieval and the efficient calculation of total column averaging kernels, ATMOSPHERIC MEASUREMENT TECHNIQUES, 7, 523–535, https://doi.org/10.5194/amt-7-523-2014, 2014.

Borsdorff, T., Aan de Brugh, J., Hu, H., Aben, I., Hasekamp, O., and Landgraf, J.: Measuring Carbon Monoxide With TROPOMI: First Results and a Comparison With ECMWF-IFS Analysis Data, GEOPHYSICAL RESEARCH LETTERS, 45, 2826–2832, https://doi.org/10.1002/2018GL077045, 2018a.

Borsdorff, T., aan de Brugh, J., Hu, H., Hasekamp, O., Sussmann, R., Rettinger, M., Hase, F., Gross, J., Schneider, M., Garcia, O., Stremme, W., Grutter, M., Feist, D. G., Arnold, S. G., De Maziere, M., Sha, M. K., Pollard, D. F., Kiel, M., Roehl, C., Wennberg, P. O., Toon, G. C., and Landgraf, J.: Mapping carbon monoxide pollution from space down to city scales with daily global coverage, ATMOSPHERIC MEASUREMENT TECHNIQUES, 11, 5507–5518, https://doi.org/10.5194/amt-11-5507-2018, 2018b.

Buchholz, R. R., Deeter, M. N., Worden, H. M., Gille, J., Edwards, D. P., Hannigan, J. W., Jones, N. B., Paton-Walsh, C., Griffith, D. W. T., Smale, D., Robinson, J., Strong, K., Conway, S., Sussmann, R., Hase, F., Blumenstock, T., Mahieu, E., and Langerock, B.: Validation of MOPITT carbon monoxide using ground-based Fourier transform infrared spectrometer data from NDACC, ATMOSPHERIC MEASUREMENT TECHNIQUES, 10, 1927–1956, https://doi.org/10.5194/amt-10-1927-2017, 2017.

Clerbaux, C., Boynard, A., Clarisse, L., George, M., Hadji-Lazaro, J., Herbin, H., Hurtmans, D., Pommier, M., Razavi, A., Turquety, S., Wespes, C., and Coheur, P. F.: Monitoring of atmospheric composition using the thermal infrared IASI/MetOp sounder, ATMOSPHERIC CHEMISTRY AND PHYSICS, 9, 6041–6054, https://doi.org/10.5194/acp-9-6041-2009, 2009.

Crosson, E. R.: A cavity ring-down analyzer for measuring atmospheric levels of methane, carbon dioxide, and water vapor, APPLIED PHYSICS B-LASERS AND OPTICS, 92, 403–408, https://doi.org/10.1007/s00340-008-3135-y, 1st International Conferene on Field Laser Applications in Industry and Research, Florence, ITALY, SEP 02-07, 2007, 2008.

Deeter, M., Emmons, L., Francis, G., Edwards, D., Gille, J., Warner, J., Khattatov, B., Ziskin, D., Lamarque, J., Ho, S., Yudin, V., Attie, J., Packman, D., Chen, J., Mao, D., and Drummond, J.: Operational carbon monoxide retrieval algorithm and selected results for the MOPITT instrument, JOURNAL OF GEOPHYSICAL RESEARCH-ATMOSPHERES, 108, https://doi.org/10.1029/2002JD003186, 2003.

Deeter, M. N.: MOPITT Measurements Of Pollution In The Troposphere validation version 4 product users guide, Tech. rep., Atmospheric Chemistry Division, National Center for Atmospheric Research, 2009.

Deeter, M. N., Worden, H. M., Gille, J. C., Edwards, D. P., Mao, D., and Drummond, J. R.: MOPITT multispectral CO retrievals: Origins and effects of geophysical radiance errors, JOURNAL OF GEOPHYSICAL RESEARCH-ATMOSPHERES, 116, https://doi.org/10.1029/2011JD015703, 2011.

Deeter, M. N., Worden, H. M., Edwards, D. P., Gille, J. C., and Andrews, A. E.: Evaluation of MOPITT retrievals of lower-tropospheric carbon monoxide over the United States, JOURNAL OF GEOPHYSICAL RESEARCH-ATMOSPHERES, 117, https://doi.org/10.1029/2012JD017553, 2012.

Deeter, M. N., Edwards, D. P., Francis, G. L., Gille, J. C., Martinez-Alonso, S., Worden, H. M., and Sweeney, C.: A climate-scale satellite record for carbon monoxide: the MOPITT Version 7 product, ATMOSPHERIC MEASUREMENT TECHNIQUES, 10, 2533–2555, https://doi.org/10.5194/amt-10-2533-2017, 2017.

https://doi.org/10.5194/amt-2020-63
Preprint. Discussion started: 6 March 2020

Deeter, M. N., Edwards, D. P., Francis, G. L., Gille, J. C., Mao, D., Martinez-Alonso, S., Worden, H. M., Ziskin, D., and Andreae, M. O.: Radiance-based retrieval bias mitigation for the MOPITT instrument: the version 8 product, ATMOSPHERIC MEASUREMENT TECHNIQUES, 12, 4561–4580, https://doi.org/10.5194/amt-12-4561-2019, 2019.

Drummond, J. and Mand, G.: The measurements of pollution in the troposphere (MOPITT) instrument: Overall performance and calibration requirements, JOURNAL OF ATMOSPHERIC AND OCEANIC TECHNOLOGY, 13, 314–320, https://doi.org/10.1175/1520-0426(1996)013<0314:TMOPIT>2.0.CO;2, 1996.

Drummond, J. R., Zou, J., Nichitiu, F., Kar, J., Deschambaut, R., and Hackett, J.: A review of 9-year performance and operation of the MOPITT instrument, ADVANCES IN SPACE RESEARCH, 45, 760–774, https://doi.org/10.1016/j.asr.2009.11.019, 2010.

ESRL: Update on the WMO X2014A CO scale July 2018, https://www.esrl.noaa.gov/gmd/ccl/co_scale_update.html, last access: 02 February 2020, 2018.

Francis, G. L., Deeter, M. N., Martínez-Alonso, S., Gille, J. C., Edwards, D. P., Mao, D., Worden, H. M., and Ziskin, D.: Measurement Of Pollution In The Troposphere algorithm theoretical basis document. Retrieval of carbon monoxide profiles and column amounts from MOPITT observed radiances (Level 1 to Level 2), Tech. rep., Atmospheric Chemistry Observations and Modeling Laboratory, National Center for Atmospheric Research, 2017.

Fu, D., Bowman, K. W., Worden, H. M., Natraj, V., Worden, J. R., Yu, S., Veefkind, P., Aben, I., Landgraf, J., Strow, L., and Han, Y.: High-resolution tropospheric carbon monoxide profiles retrieved from CrIS and TROPOMI, ATMOSPHERIC MEASUREMENT TECHNIQUES, 9, 2567–2579, https://doi.org/10.5194/amt-9-2567-2016, 2016.

George, M., Clerbaux, C., Hurtmans, D., Turquety, S., Coheur, P. F., Pommier, M., Hadji-Lazaro, J., Edwards, D. P., Worden, H., Luo, M., Rinsland, C., and McMillan, W.: Carbon monoxide distributions from the IASI/METOP mission: evaluation with other space-borne remote sensors, ATMOSPHERIC CHEMISTRY AND PHYSICS, 9, 8317–8330, https://doi.org/10.5194/acp-9-8317-2009, 2009.

George, M., Clerbaux, C., Bouarar, I., Coheur, P. F., Deeter, M. N., Edwards, D. P., Francis, G., Gille, J. C., Hadji-Lazaro, J., Hurtmans, D., Inness, A., Mao, D., and Worden, H. M.: An examination of the long-term CO records from MOPITT and IASI: comparison of retrieval methodology, ATMOSPHERIC MEASUREMENT TECHNIQUES, 8, 4313–4328, https://doi.org/10.5194/amt-8-4313-2015, 2015.

Giglio, L., Csiszar, I., and Justice, C. O.: Global distribution and seasonality of active fires as observed with the Terra and Aqua Moderate Resolution Imaging Spectroradiometer (MODIS) sensors, JOURNAL OF GEOPHYSICAL RESEARCH-BIOGEOSCIENCES, 111, https://doi.org/10.1029/2005JG000142, 2006.

Heald, C., Jacob, D., Fiore, A., Emmons, L., Gille, J., Deeter, M., Warner, J., Edwards, D., Crawford, J., Hamlin, A., Sachse, G., Browell, E., Avery, M., Vay, S., Westberg, D., Blake, D., Singh, H., Sandholm, S., Talbot, R., and Fuelberg, H.: Asian outflow and trans-Pacific transport of carbon monoxide and ozone pollution: An integrated satellite, aircraft, and model perspective, JOURNAL OF GEOPHYSICAL RESEARCH-ATMOSPHERES, 108, https://doi.org/10.1029/2003JD003507, 2003.

Hedelius, J. K., He, T.-L., Jones, D. B. A., Baier, B. C., Buchholz, R. R., De Maziere, M., Deutscher, N. M., Dubey, M. K., Feist, D. G., Griffith, D. W. T., Hase, F., Iraci, L. T., Jeseck, P., Kiel, M., Kivi, R., Liu, C., Morino, I., Notholt, J., Oh, Y.-S., Ohyama, H., Pollard, D. F., Rettinger, M., Roche, S., Roehl, C. M., Schneider, M., Shiomi, K., Strong, K., Sussmann, R., Sweeney, C., Te, Y., Uchino, O., Velazco, V. A., Wang, W., Warneke, T., Wennberg, P. O., Worden, H. M., and Wunch, D.: Evaluation of MOPITT Version 7 joint TIR-NIR X-CO retrievals with TCCON, ATMOSPHERIC MEASUREMENT TECHNIQUES, 12, 5547–5572, https://doi.org/10.5194/amt-12-5547-2019, 2019.

Holloway, T., Levy, H., and Kasibhatla, P.: Global distribution of carbon monoxide, JOURNAL OF GEOPHYSICAL RESEARCH-ATMOSPHERES, 105, 12 123–12 147, https://doi.org/10.1029/1999JD901173, 2000.

https://doi.org/10.5194/amt-2020-63
Preprint. Discussion started: 6 March 2020

Karion, A., Sweeney, C., Wolter, S., Newberger, T., Chen, H., Andrews, A., Kofler, J., Neff, D., and Tans, P.: Long-term greenhouse gas measurements from aircraft, ATMOSPHERIC MEASUREMENT TECHNIQUES, 6, 511–526, https://doi.org/10.5194/amt-6-511-2013, 2013.

Krol, M., Houweling, S., Bregman, B., van den Broek, M., Segers, A., van Velthoven, P., Peters, W., Dentener, F., and Bergamaschi, P.: The two-way nested global chemistry-transport zoom model TM5: algorithm and applications, ATMOSPHERIC CHEMISTRY AND PHYSICS, 5, 417–432, https://doi.org/10.5194/acp-5-417-2005, 2005.

Lamarque, J. F., Emmons, L. K., Hess, P. G., Kinnison, D. E., Tilmes, S., Vitt, F., Heald, C. L., Holland, E. A., Lauritzen, P. H., Neu, J., Orlando, J. J., Rasch, P. J., and Tyndall, G. K.: CAM-chem: description and evaluation of interactive atmospheric chemistry in the Community Earth System Model, GEOSCIENTIFIC MODEL DEVELOPMENT, 5, 369–411, https://doi.org/10.5194/gmd-5-369-2012, 2012.

Landgraf, J., aan de Brugh, J., Scheepmaker, R., Borsdorff, T., Hu, H., Houweling, S., Butz, A., Aben, I., and Hasekamp, O.: Carbon monoxide total column retrievals from TROPOMI shortwave infrared measurements, ATMOSPHERIC MEASUREMENT TECHNIQUES, 9, 4955–4975, https://doi.org/10.5194/amt-9-4955-2016, 2016.

Landgraf, J., Borsdorff, T., Langerock, B., and Keppens, A.: S5P mission performance centre carbon monoxide (L2 CO) readme, Tech. Rep. 1.0.0, 2018-07-09, Netherlands Institute for Space Research (SRON), 2018.

Lelieveld, J., Gromov, S., Pozzer, A., and Taraborrelli, D.: Global tropospheric hydroxyl distribution, budget and reactivity, ATMOSPHERIC CHEMISTRY AND PHYSICS, 16, 12 477–12 493, https://doi.org/10.5194/acp-16-12477-2016, 2016.

Martínez-Alonso, S., Deeter, M. N., Worden, H. M., Gille, J. C., Emmons, L. K., Pan, L. L., Park, M., Manney, G. L., Bernath, P. F., Boone, C. D., Walker, K. A., Kolonjari, F., Wofsy, S. C., Pittman, J., and Daube, B. C.: Comparison of upper tropospheric carbon monoxide from MOPITT, ACE-FTS, and HIPPO-QCLS, JOURNAL OF GEOPHYSICAL RESEARCH-ATMOSPHERES, 119, 14 144–14 164, https://doi.org/10.1002/2014JD022397, 2014.

McKain, K. and Sweeney, C.: Readme for NOAA-Picarro on ATom-1,2,3,4, Tech. rep., Cooperative Institute for Research in the Environmental Sciences, University of Colorado and NOAA Earth System Research Laboratory, 2018.

McManus, J. B., Zahniser, M. S., Nelson, Jr., D. D., Shorter, J. H., Herndon, S., Wood, E., and Wehr, R.: Application of quantum cascade lasers to high-precision atmospheric trace gas measurements, OPTICAL ENGINEERING, 49, https://doi.org/10.1117/1.3498782, 2010.

Myhre, G., Shindell, D., Bréon, F.-M., Collins, W., Fuglestvedt, J., Huang, J., Koch, D., Lamarque, J.-F., Lee, D., Mendoza, B., Nakajima, T., Robock, A., Stephens, G., Takemura, T., and Zhang, H.: Anthropogenic and natural radiative forcing, pp. 659–740, Cambridge University Press, Cambridge, UK, https://doi.org/10.1017/CBO9781107415324.018, 2013.

Rodgers, C. and Connor, B.: Intercomparison of remote sounding instruments, JOURNAL OF GEOPHYSICAL RESEARCH-ATMOSPHERES, 108, https://doi.org/10.1029/2002JD002299, 2003.

Santoni, G. W., Daube, B. C., Kort, E. A., Jimenez, R., Park, S., Pittman, J. V., Gottlieb, E., Xiang, B., Zahniser, M. S., Nelson, D. D., McManus, J. B., Peischl, J., Ryerson, T. B., Holloway, J. S., Andrews, A. E., Sweeney, C., Hall, B., Hintsa, E. J., Moore, F. L., Elkins, J. W., Hurst, D. F., Stephens, B. B., Bent, J., and Wofsy, S. C.: Evaluation of the airborne quantum cascade laser spectrometer (QCLS) measurements of the carbon and greenhouse gas suite - CO2, CH4, N2O, and CO - during the CalNex and HIPPO campaigns, ATMOSPHERIC MEASUREMENT TECHNIQUES, 7, 1509–1526, https://doi.org/10.5194/amt-7-1509-2014, 2014.

Spivakovsky, C., Logan, J., Montzka, S., Balkanski, Y., Foreman-Fowler, M., Jones, D., Horowitz, L., Fusco, A., Brenninkmeijer, C., Prather, M., Wofsy, S., and McElroy, M.: Three-dimensional climatological distribution of tropospheric OH: Update and evaluation, JOURNAL OF GEOPHYSICAL RESEARCH-ATMOSPHERES, 105, 8931–8980, https://doi.org/10.1029/1999JD901006, 2000.

https://doi.org/10.5194/amt-2020-63
Preprint. Discussion started: 6 March 2020

Atmospheric Measurement Techniques Discussions

Veefkind, J. P., Aben, I., McMullan, K., Forster, H., de Vries, J., Otter, G., Claas, J., Eskes, H. J., de Haan, J. F., Kleipool, Q., van Weele, M., Hasekamp, O., Hoogeveen, R., Landgraf, J., Snel, R., Tol, P., Ingmann, P., Voors, R., Kruizinga, B., Vink, R., Visser, H., and Levelt, P. F.: TROPOMI on the ESA Sentinel-5 Precursor: A GMES mission for global observations of the atmospheric composition for climate, air quality and ozone layer applications, REMOTE SENSING OF ENVIRONMENT, 120, 70–83, https://doi.org/10.1016/j.rse.2011.09.027, 2012.

Vidot, J., Landgraf, J., Hasekamp, O. P., Butz, A., Galli, A., Tol, P., and Aben, I.: Carbon monoxide from shortwave infrared reflectance measurements: A new retrieval approach for clear sky and partially cloudy atmospheres, REMOTE SENSING OF ENVIRONMENT, 120, 255–266, https://doi.org/10.1016/j.rse.2011.09.032, 2012.

Wofsy, S., Afshar, S., Allen, H., Apel, E., Asher, E., Barletta, B., Bent, J., Bian, H., Biggs, B., Blake, D., Blake, N., Bourgeois, I., Brock, C., Brune, W., Budney, J., Bui, T., Butler, A., Campuzano-Jost, P., Chang, C., Chin, M., Commane, R., Correa, G., Crounse, J., Cullis, P., Daube, B., Day, D., Dean-Day, J., Dibb, J., Digangi, J., Diskin, G., Dollner, M., Elkins, J., Erdesz, F., Fiore, A., Flynn, C., Froyd, K., Gesler, D., Hall, S., Hanisco, T., Hannun, R., Hills, A., Hintsa, E., Hoffman, A., Hornbrook, R., Huey, L., Hughes, S., Jimenez, J., Johnson, B., Katich, J., Keeling, R., Kim, M., Kupc, A., Lait, L., Lamarque, J.-F., Liu, J., Mckain, K., Mclaughlin, R., Meinardi, S., Miller, D., Montzka, S., Moore, F., Morgan, E., Murphy, D., Murray, L., Nault, B., Neuman, J., Newman, P., Nicely, J., Pan, X., Paplawsky, W., Peischl, J., Prather, M., Price, D., Ray, E., Reeves, J., Richardson, M., Rollins, A., Rosenlof, K., Ryerson, T., Scheuer, E., Schill, G., Schroder, J., Schwarz, J., St.Clair, J., Steenrod, S., Stephens, B., Strode, S., Sweeney, C., Tanner, D., Teng, A., Thames, A., Thompson, C., Ullmann, K., Veres, P., Vizenor, N., Wagner, N., Watt, A., Weber, R., Weinzierl, B., Wennberg, P., Williamson, C., Wilson, J., Wolfe, G., Woods, C., and Zeng, L.: ATom: Merged Atmospheric Chemistry, Trace Gases, and Aerosols, https://doi.org/10.3334/ORNLDAAC/1581, 2018.

Worden, H. M., Deeter, M. N., Edwards, D. P., Gille, J. C., Drummond, J. R., and Nedelec, P.: Observations of near-surface carbon monoxide from space using MOPITT multispectral retrievals, JOURNAL OF GEOPHYSICAL RESEARCH-ATMOSPHERES, 115, https://doi.org/10.1029/2010JD014242, 2010.

Worden, H. M., Deeter, M. N., Edwards, D. P., Gille, J., Drummond, J., Emmons, L. K., Francis, G., and Martinez-Alonso, S.: 13 years of MOPITT operations: lessons from MOPITT retrieval algorithm development, ANNALS OF GEOPHYSICS, 56, https://doi.org/10.4401/ag-6330, 2013a.

Worden, H. M., Deeter, M. N., Frankenberg, C., George, M., Nichitiu, F., Worden, J., Aben, I., Bowman, K. W., Clerbaux, C., Coheur, P. F., de Laat, A. T. J., Detweiler, R., Drummond, J. R., Edwards, D. P., Gille, J. C., Hurtmans, D., Luo, M., Martinez-Alonso, S., Massie, S., Pfister, G., and Warner, J. X.: Decadal record of satellite carbon monoxide observations, ATMOSPHERIC CHEMISTRY AND PHYSICS, 13, 837–850, https://doi.org/10.5194/acp-13-837-2013, 2013b.

https://doi.org/10.5194/amt-2020-63
Preprint. Discussion started: 6 March 2020

Atmospheric Measurement Techniques Discussions

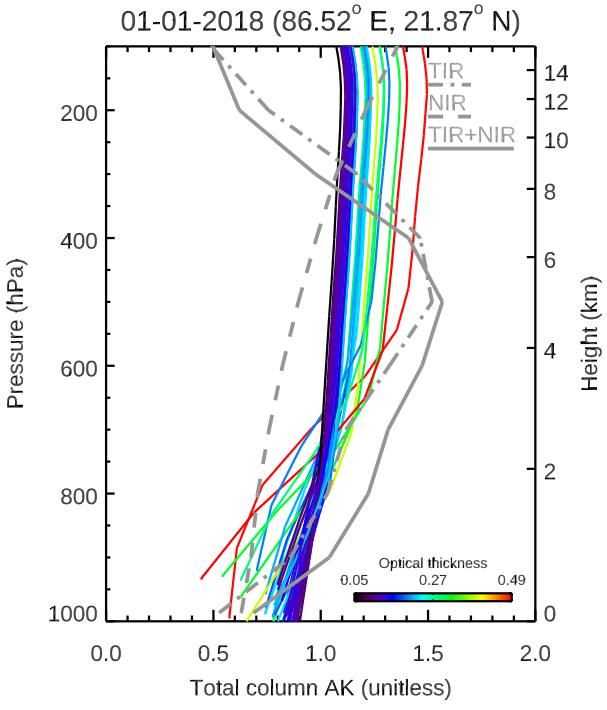

Figure 1. Total column AK (averaging kernels) from MOPITT and TROPOMI observations acquired 1 January 2018. Gray lines show AK from a single clear MOPITT pixel. Color-coded lines show AK from TROPOMI observations colocated with that MOPITT pixel (same day acquisition, $\leq$ 50 km horizontal distance) with optical depth <0.5 and cloud height <5000 m (i.e., clear-sky, clear-sky-like, and mid-level-cloud observations). Differences in TROPOMI AK vertical extent are due to topography.

https://doi.org/10.5194/amt-2020-63
Preprint. Discussion started: 6 March 2020

Atmospheric Measurement Techniques Discussions

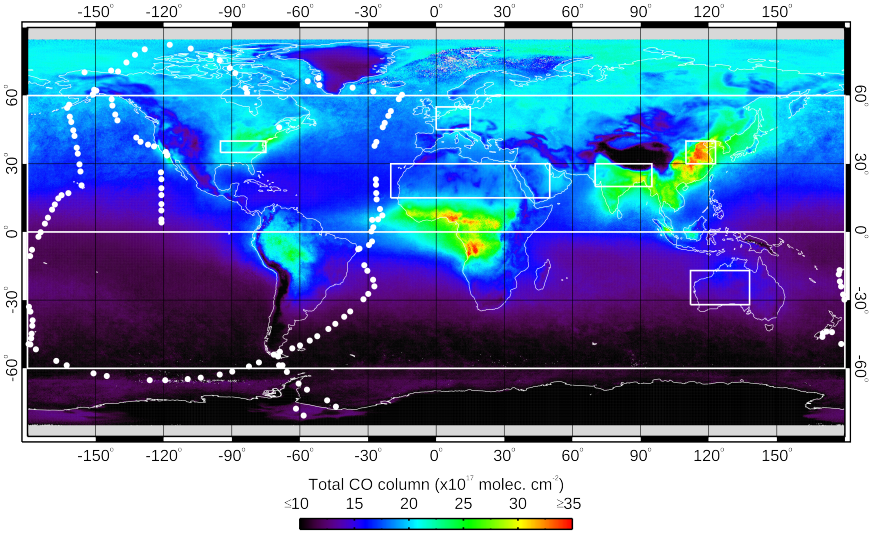

Figure 2. White rectangles show the location of land-only ROIs analyzed: N Hemisphere (0°N to 60°N), S Hemisphere (60°S to 0°N), USA (35°N, 95°W to 40°N, 75°W), Europe (45°N, 0°E to 55°N, 15°E), India (20°N, 70°E to 30°N, 95°E), China (30°N, 110°E to 40°N, 123°E), Sahara (15°N, 20°W to 30°N, 50°E), and Australia (32°S, 112°E to 17°S, 138°E). White circles indicate location of individual CO profiles acquired in April-May 2018, during the ATom-4 airborne campaign. Background map shows mean MOPITT TIR total CO column values for 2018.

https://doi.org/10.5194/amt-2020-63
Preprint. Discussion started: 6 March 2020

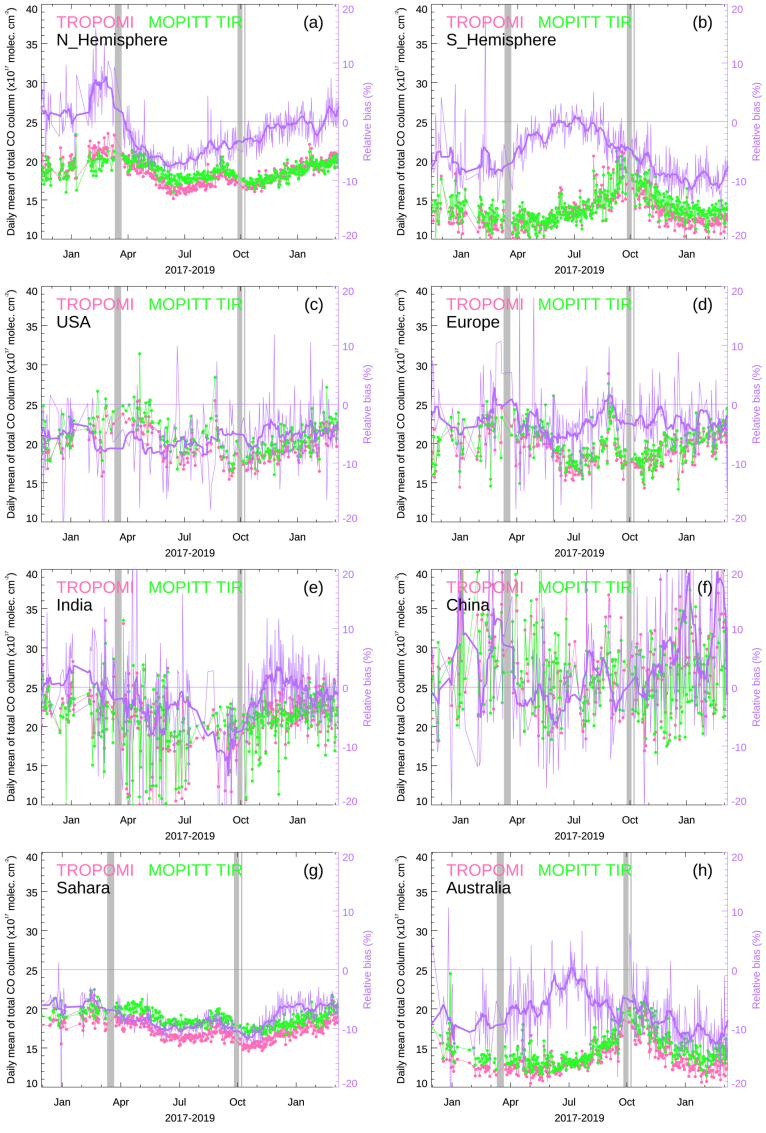

Figure 3. Comparison of colocated land retrievals from TROPOMI (pink) and MOPITT TIR (green) for each ROI analyzed. Filled circles show daily mean. Thin purple lines indicate daily relative bias (i.e., accuracy) between the two datasets, thick purple lines are a 11-day smoothed version with high-frequency variability removed. Gray bars show periods without MOPITT measurements because of hot calibrations (March and October 2018) or a safe mode maneuver (October-November 2018).

https://doi.org/10.5194/amt-2020-63
Preprint. Discussion started: 6 March 2020

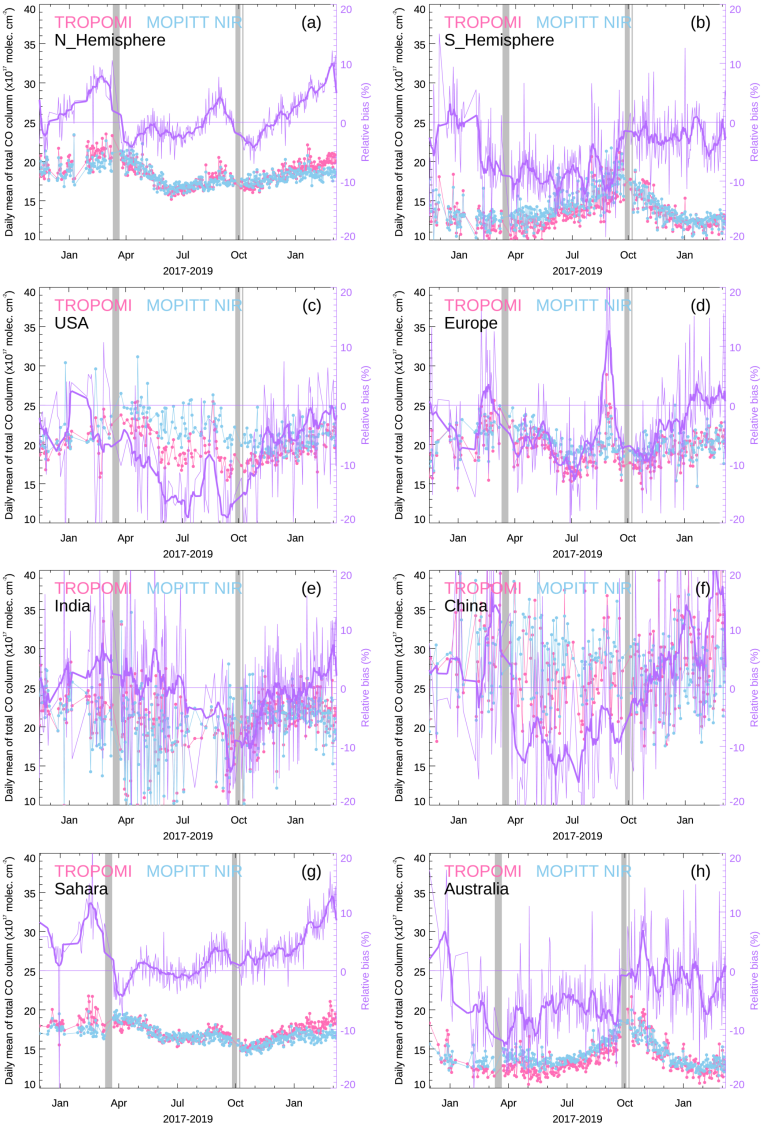

Figure 4. Comparison of colocated land retrievals from TROPOMI (pink) and MOPITT NIR (blue) for each ROI analyzed. See caption to Fig. 3 for details.

https://doi.org/10.5194/amt-2020-63
Preprint. Discussion started: 6 March 2020

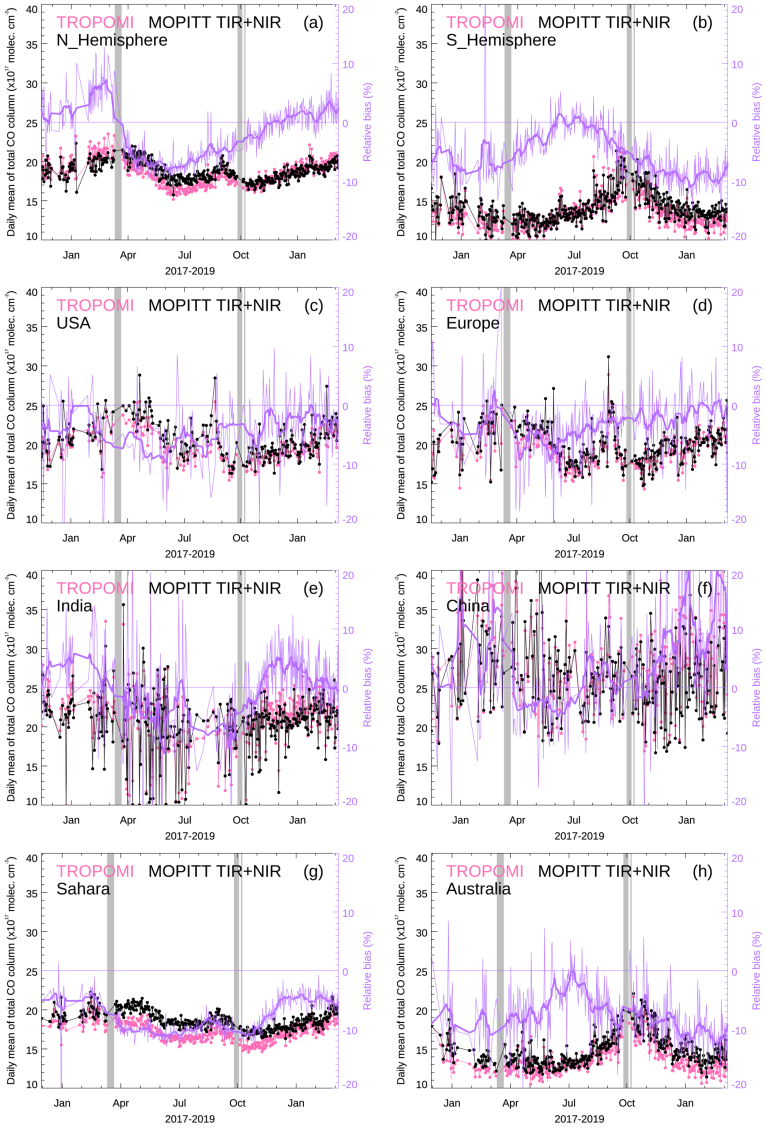

Figure 5. Comparison of colocated land retrievals from TROPOMI (pink) and MOPITT TIR+NIR (black) for each ROI analyzed. See caption to Fig. 3 for details.

https://doi.org/10.5194/amt-2020-63
Preprint. Discussion started: 6 March 2020

Atmospheric Measurement Techniques Discussions

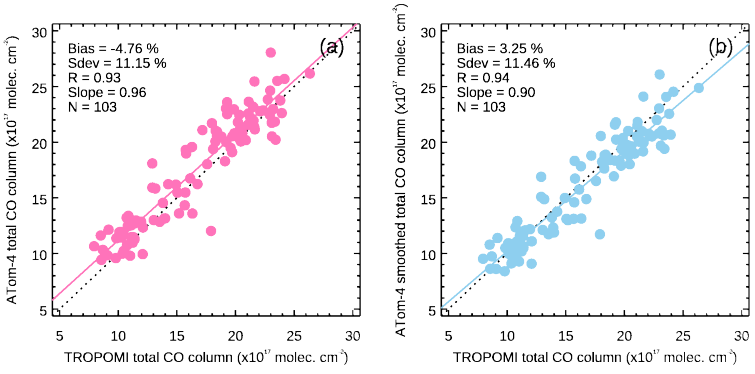

Figure 6. Comparison of colocated retrievals over bodies of water from TROPOMI and ATom-4 (24 April - 21 May 2018). a) TROPOMI versus true (unsmoothed) ATom-4. b) TROPOMI versus retrieval-simulated (smoothed) ATom-4.

https://doi.org/10.5194/amt-2020-63
Preprint. Discussion started: 6 March 2020

Atmospheric Measurement Techniques Discussions

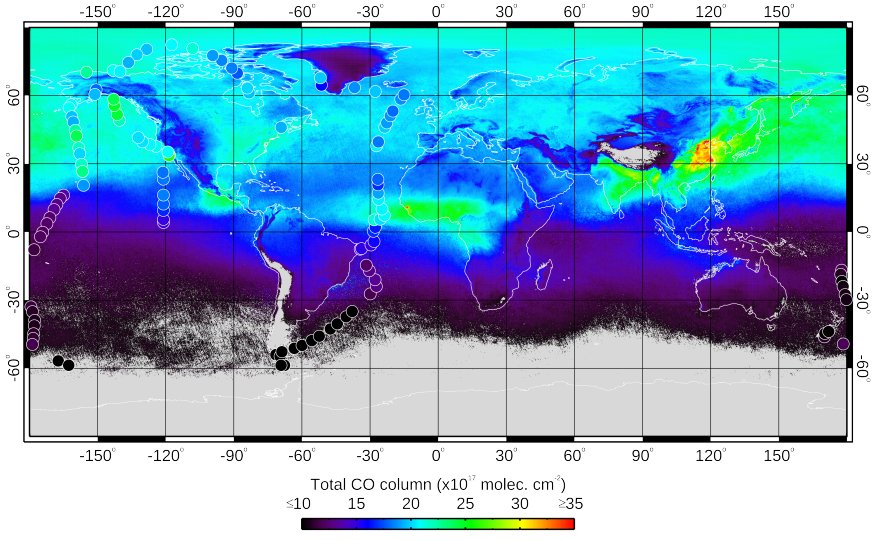

Figure 7. Map of averaged TROPOMI total CO column values acquired between 24 April and 21 May 2018, the duration of the ATom-4 campaign. Circles show ATom-4 profiles spatially and temporally colocated with single TROPOMI retrievals; circles are color-coded according to their retrieval-simulated (smoothed) ATom total CO column value. There is good agreement between the two datasets, despite differences in the time span and footprint size each of them represents.

https://doi.org/10.5194/amt-2020-63
Preprint. Discussion started: 6 March 2020

Atmospheric Measurement Techniques Discussions

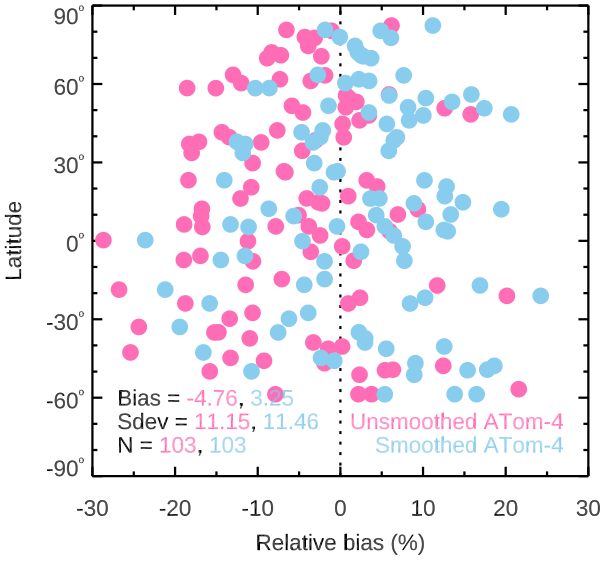

Figure 8. Latitudinal distribution of relative bias between TROPOMI and ATom-4 over bodies of water. Negative bias indicates that TROPOMI retrievals are low with respect to ATom-4.

https://doi.org/10.5194/amt-2020-63
Preprint. Discussion started: 6 March 2020

Atmospheric Measurement Techniques Discussions

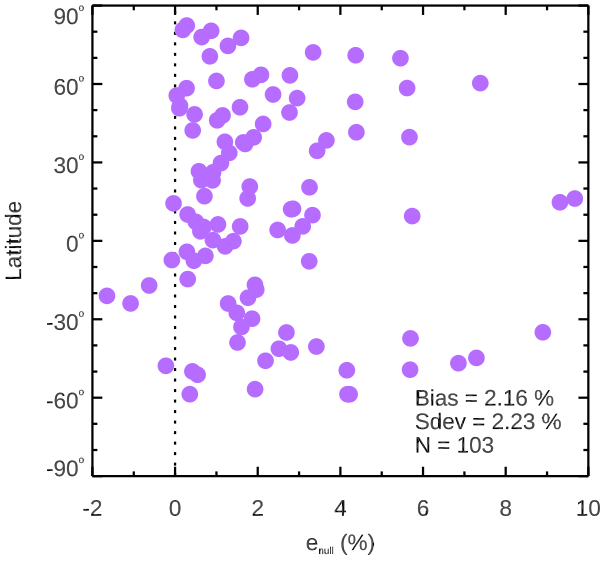

Figure 9. Latitudinal distribution of e_{null} error (see Eq. (4)), which characterizes retrieval errors over cloudy scenes related to the shape of the TROPOMI model-calculated reference profiles, expressed in percentage with respect to the true (unsmoothed) ATom-4 total CO columns.

https://doi.org/10.5194/amt-2020-63
Preprint. Discussion started: 6 March 2020

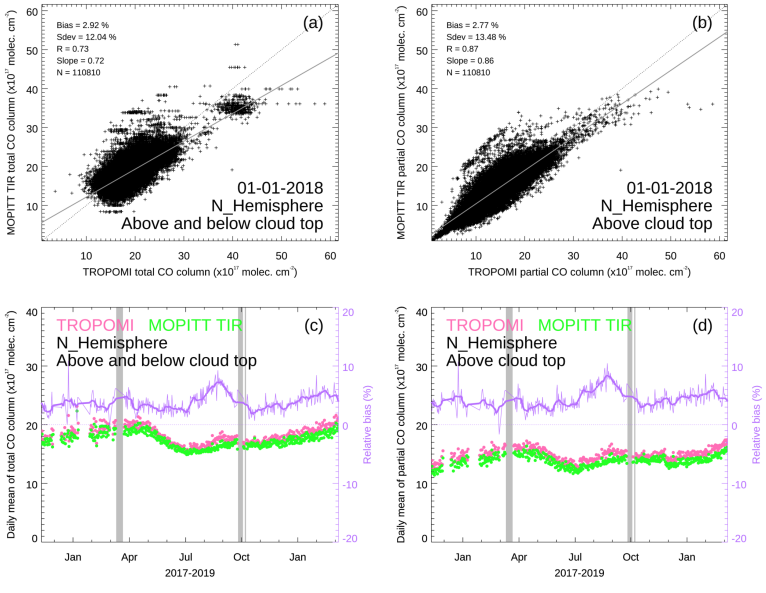

Figure 10. Comparison of colocated retrievals over bodies of water from TROPOMI and MOPITT TIR for the N Hemisphere ROI. a) Total CO column values (above and below cloud top) for a single day, 1 January 2018. b) Partial CO column values (above-cloud only) for the same day. c) Compilation of means and relative biases of total CO column values (above and below cloud top) from 7 November 2017 to 10 March 2019. d) Same for partial CO column values (above-cloud only).

https://doi.org/10.5194/amt-2020-63
Preprint. Discussion started: 6 March 2020

Atmospheric Measurement Techniques Discussions

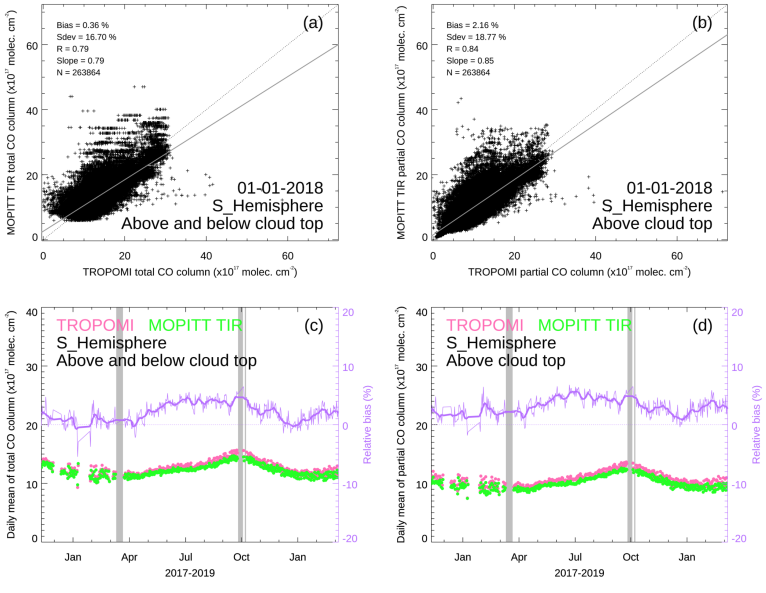

Figure 11. Comparison of colocated retrievals over bodies of water from TROPOMI and MOPITT TIR for the S Hemisphere ROI. a) Total CO column values (above and below cloud top) for a single day, 1 January 2018. b) Partial CO column values (above-cloud only) for the same day. c) Compilation of means and relative biases of total CO column values (above and below cloud top) from 7 November 2017 to 10 March 2019. d) Same for partial CO column values (above-cloud only).

https://doi.org/10.5194/amt-2020-63
Preprint. Discussion started: 6 March 2020

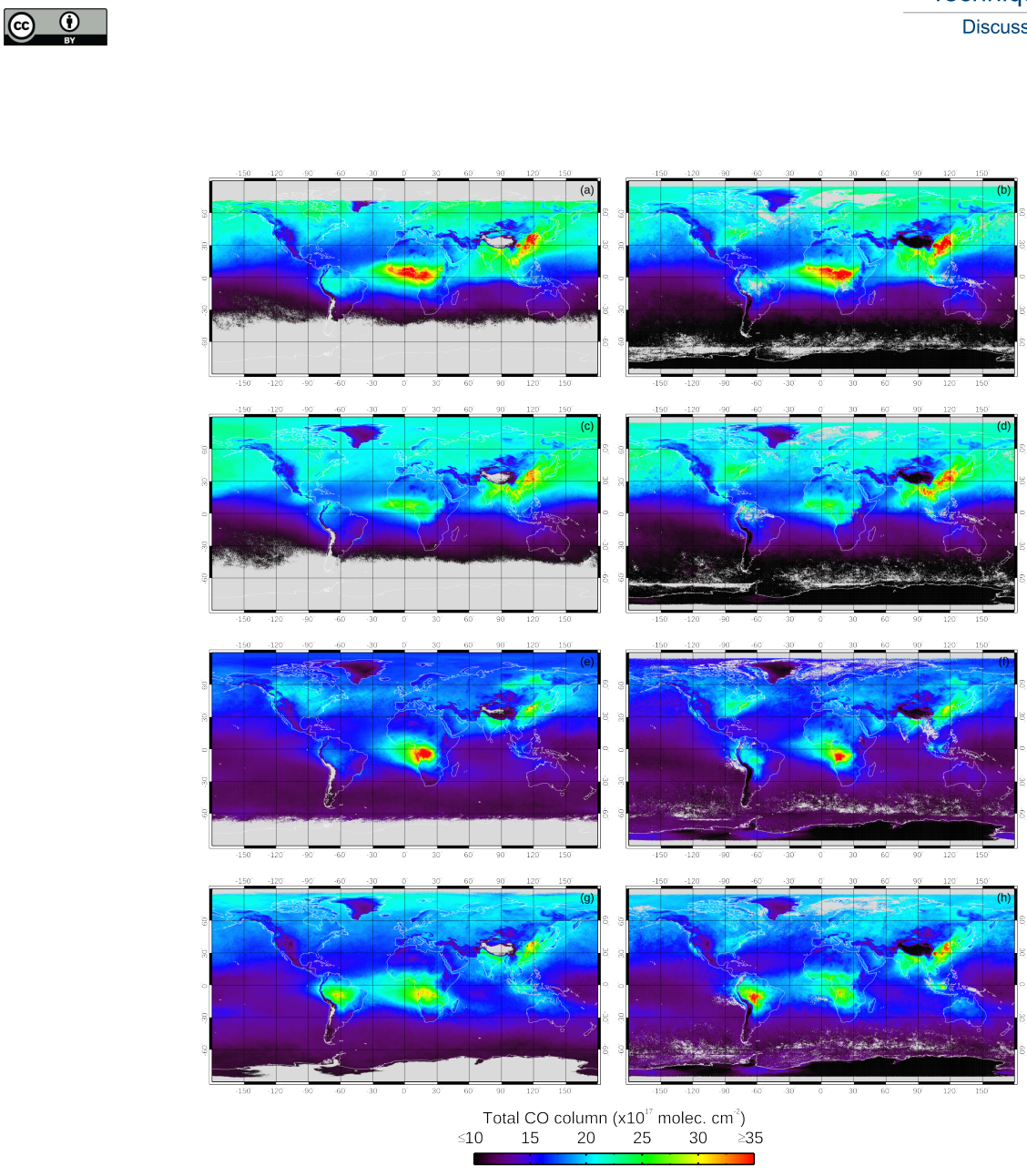

Figure 12. Seasonal averages of TROPOMI and MOPITT TIR CO retrievals. a) December 2017 to February 2018 (DJF) TROPOMI mean. b) Same for MOPITT. c) March-May 2018 (MAM) TROPOMI mean. d) Same for MOPITT. e) June-August 2018 (JJA) TROPOMI mean. f) Same for MOPITT. g) September-November 2018 (SON) TROPOMI mean. h) Same for MOPITT. Sharp discontinuities visible in some panels at 65°S are due to differences in the definition of the MOPITT cloud mask poleward of latitude 65°.

https://doi.org/10.5194/amt-2020-63
Preprint. Discussion started: 6 March 2020

Atmospheric Measurement Techniques Discussions

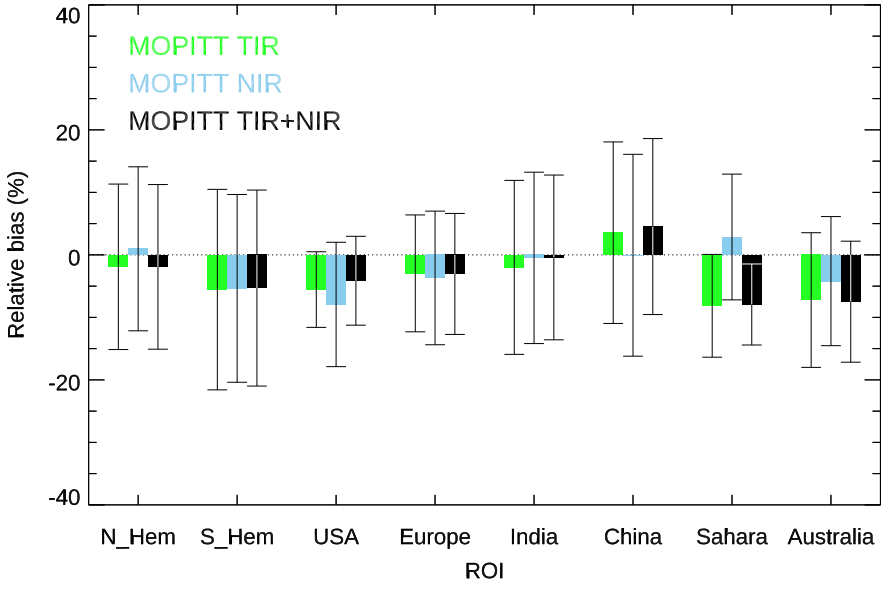

Figure 13. Summary of colocated land comparison results. Colored bars represent relative bias between TROPOMI and each of the three MOPITT products (TIR, NIR, and TIR+NIR); solid lines indicate the standard deviation of relative bias

https://doi.org/10.5194/amt-2020-63
Preprint. Discussion started: 6 March 2020

Atmospheric Measurement Techniques Discussions

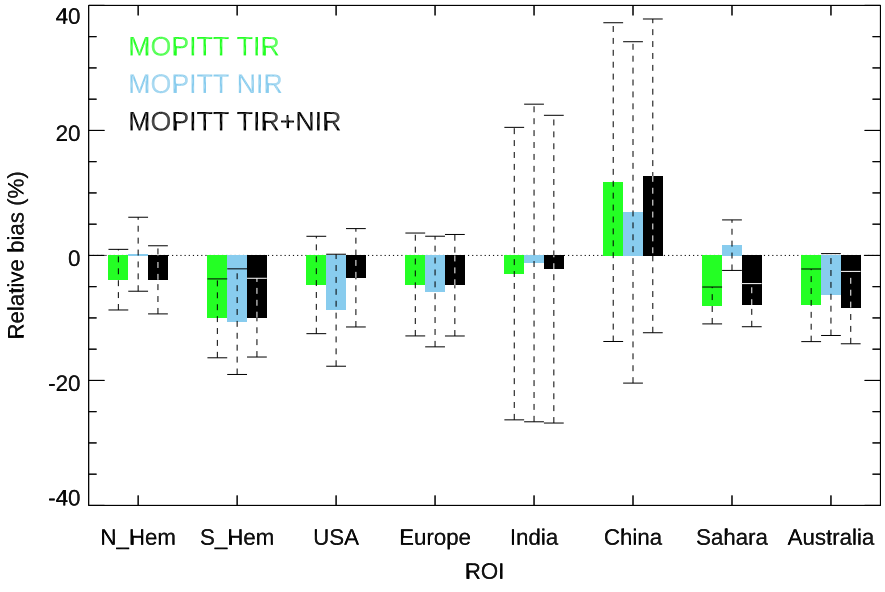

Figure 14. Summary of non-colocated land comparison results. Colored bars represent relative bias between TROPOMI and each of the three MOPITT products (TIR, NIR, and TIR+NIR). Solid lines show ± 1 standard deviation of mean daily relative biases (i.e., inter-daily bias variability).

https://doi.org/10.5194/amt-2020-63
Preprint. Discussion started: 6 March 2020

Atmospheric Measurement Techniques Discussions

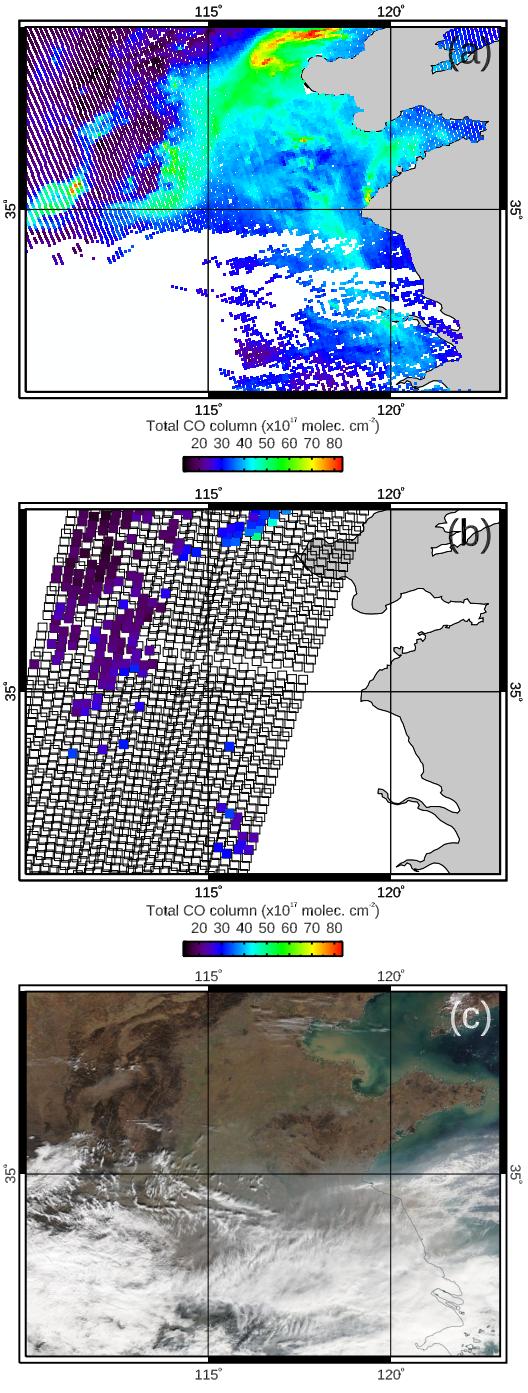

Figure 15. Total CO column retrievals and visible image for the China ROI on 1 January 2018. a) TROPOMI map. b) MOPITT TIR+NIR map. c) Terra-MODIS visible image acquired at the same time as the MOPITT data. Empty boxes in the second panel correspond to MOPITT observations deemed cloudy based on MODIS cloud mask information, and thus not suitable for CO retrieval. The MODIS visible image shows clouds in the southern half of the ROI; the northern half was hazy, most probably due to pollution, but cloud-free.

https://doi.org/10.5194/amt-2020-63
Preprint. Discussion started: 6 March 2020

Atmospheric Measurement Techniques Discussions

Table 1. Statistics from colocated TROPOMI versus MOPITT CO retrievals over land for the period between 7 November 2017 and 10 March 2019. Relative bias and standard deviation in %. Column bias and standard deviation in units of 10^{17} molec. cm^{-2}.

		TROPOMI vs $MOPITT_{TIR}$	TROPOMI vs $MOPITT_{NIR}$	TROPOMI vs $MOPITT_{TIR+NIR}$
N Hemisphere	Relative Bias±St. Dev.	-1.91±13.24	0.97±13.12	-1.92±13.17
	Column Bias±St. Dev.	–0.55±2.51	-0.04±2.58	-0.55±2.45
	Mean Daily Colocated Pairs	45672	45678	45530
S Hemisphere	Relative Bias±St. Dev.	-5.56±16.04	-5.36±15.02	-5.31±15.68
	Column Bias±St. Dev.	-1.02±2.50	-0.95±2.32	-0.95±2.30
	Mean Daily Colocated Pairs	7768	7771	7748
USA	Relative Bias±St. Dev.	-5.55±6.05	-7.93±9.95	-4.14±7.11
	Column Bias±St. Dev.	-1.25±1.33	-2.02±2.36	-1.00±1.53
	Mean Daily Colocated Pairs	666	686	666
Europe	Relative Bias±St. Dev.	-2.96±9.35	-3.69±10.69	-3.05±9.68
	Column Bias±St. Dev.	-0.73±1.84	-0.91±2.29	-0.79±2.04
	Mean Daily Colocated Pairs	657	661	656
India	Relative Bias±St. Dev.	-2.00±13.92	-0.48±13.71	-0.41±13.18
	Column Bias±St. Dev.	-0.74±2.80	-0.47±2.90	-0.38±2.43
	Mean Daily Colocated Pairs	1122	1133	1118
China	Relative Bias±St. Dev.	3.55±14.52	-0.06±16.15	4.53±14.08
	Column Bias±St. Dev.	0.74±4.00	-0.37±4.64	0.98±3.86
	Mean Daily Colocated Pairs	533	566	534
Sahara	Relative Bias±St. Dev.	-8.15±8.22	2.86±10.06	-7.94±6.48
	Column Bias±St. Dev.	-1.64±1.64	0.34±1.72	-1.55±1.27
	Mean Daily Colocated Pairs	15214	15223	15169
Australia	Relative Bias±St. Dev.	-7.23±10.77	-4.20±10.33	-7.49±9.68
	Column Bias±St. Dev.	-1.28±1.85	-0.69±1.52	-1.26±1.57
	Mean Daily Colocated Pairs	1873	1875	1869
Mean all ROIs	Relative Bias±St. Dev.	-3.73±11.51	-2.24±12.38	-3.22±11.13
	Column Bias±St. Dev.	-0.81±2.31	-0.64±2.54	-0.69±2.18
	Mean Daily Colocated Pairs	9188	9199	9161

https://doi.org/10.5194/amt-2020-63
Preprint. Discussion started: 6 March 2020

Atmospheric Measurement Techniques Discussions

Table 2. Colocated TROPOMI versus ATom-4 CO retrievals over bodies of water: Statistics from AK analysis. Relative bias and standard deviation in %. Column bias and standard deviation in units of 10^{17} molec. cm^{-2}.

		TROPOMI vs True ATom-4 (Unsmoothed)	TROPOMI vs Retrieval-Simulated ATom-4 (Smoothed)
Atlantic/Pacific	Relative Bias±St. Dev.	-4.76±11.15	3.25±11.46
	Column Bias±St. Dev.	-0.89±1.80	0.46±1.68
	Number of Colocated Pairs	103	103

https://doi.org/10.5194/amt-2020-63
Preprint. Discussion started: 6 March 2020

Atmospheric Measurement Techniques Discussions

Table 3. Colocated TROPOMI versus MOPITT TIR CO retrievals over bodies of water: Statistics from above/below cloud analysis performed for the period between 7 November 2017 and 10 March 2019. Total column = above and below cloud top. Partial column = above cloud top. Relative bias and standard deviation in %. Column bias and standard deviation in units of 10^{17} molec. cm^{-2}.

		TROPOMI vs $MOPITT_{TIR}$ Total Column	TROPOMI vs $MOPITT_{TIR}$ Partial Column
N Hemisphere	Relative Bias±St. Dev.	3.82±13.27	4.35±14.72
	Column Bias±St. Dev.	0.53±2.35	0.48±2.04
	Mean Daily Colocated Pairs	127360	127360
	Change in Relative Bias (p.p.)	-0.53	
S Hemisphere	Relative Bias±St. Dev.	2.14±18.15	3.16±21.49
	Column Bias±St. Dev.	0.19±2.38	0.24±2.14
	Mean Daily Colocated Pairs	164935	164935
	Change in Relative Bias (p.p.)	-1.02	
Mean both Hemispheres	Relative Bias, St. Dev.	2.98±15.71	3.76±18.11
	Column Bias±St. Dev.	0.36±2.37	0.36±2.09
	Mean Daily Colocated Pairs	146148	146148
	Change in Relative Bias (p.p.)	-0.78	